Geospatial approaches of deriving hydro-morphological information for flood hazard management

Ph. D. Thesis

by

DIGANTA BARMAN

Department of Civil Engineering
Indian Institute of Technology Guwahati
Assam, India
November 2013

Ph. D.
Thesis

Geospatial approaches of deriving hydro-morphological information for flood hazard Management

D. Barman

2013

Geospatial approaches of deriving hydro-morphological information for flood hazard management

A Thesis

Submitted in Partial Fulfillment of the
Requirements for the Degree of

DOCTOR OF PHILOSOPHY

by

DIGANTA BARMAN

Department of Civil Engineering
Indian Institute of Technology Guwahati
Assam, India
November 2013

Chapter 1

INTRODUCTION

1.1. PURPOSE OF STUDY

Most of the river basins in developing world, even today are either ungauged or very inadequately gauged. This is a fact true for both hydrological and meteorological observations. In such a situation, it is always very difficult to calibrate and validate most of the mathematical models used for forecasting rainfall as well as runoff. Moreover, it is apparent from whatever hydrological records that are documented (in departmental annual reports, Master plans etc) in recent years, that the relevant agencies always prefer to collect the river gauge data rather than the discharge data since measurement of discharge involves tedious process in absence of modern devices. Non-availability of up-to-date river cross section data also adds to the complexities of discharge measurements by indirect methods like use of stage-discharge relationship (Rating curve) where discharge is estimated based on observed river stage. Similarly for meteorological observations, it has been found that majority of the rain gauges remain non-functional due to various logistics and technical issues. Moreover due to paucity of fund, installed rain gauges are generally ordinary measuring cylinders or at most tipping bucket type and therefore the data from these rain gauges are not of much use for real time forecasting of flow due to absence of any telemetric arrangements in them.

The North Eastern Region of India is known to be one of the most water resource rich regions in the world. This relatively small region houses two major

river valleys namely the Brahmaputra and the Barak with their host of tributaries. Along with their enormous water resources potential, there lies the fury of flood almost every year. Mitigation of flood damage has been a major challenge due to lack of an efficient flood forecasting system. Modern Automatic Weather Stations (AWS) from different governmental agencies are very less (*with respect to the guidelines of* ***World Meteorological Organization*** *regarding adequacy of rain gauge density for hilly and plain area*) in the Brahmaputra and Barak valley flood plains. With these logistics and technical constraints, the sophisticated ideal flood forecasting systems as available in developed countries do not seem to becoming a reality in the flood plains of these river valleys in near future.

In recent times advancements in various geo-spatial technologies like satellite meteorology, optical and microwave remote sensing, Geographic Information System etc. have opened doors for various cost-effective alternative scientific methods for risk reduction for management of flood disasters. Meteorological radars in various forms have assisted weather predictions from more than a decade back. Battan in 1973 has done introductory work on basics of radar based rainfall observations. Similarly Jayakrishnan *et al.* 2004 has studied about accuracy issues related to radar measurement of rainfall. Numerical rainfall prediction started developing from late eighties. The Centre for Analysis and Prediction of Storms, University of Oklahoma, USA has done pioneering work in the field of numerical weather prediction from 1989 onward. In relatively recent times, Xue *et al.* 2002 carried out a unique multi-model mesoscale ensemble prediction experiment. Ahrens and Maidment in 1999 *and* Anderson *et al.* 2002 have worked on integration of Numerical Rainfall Prediction model and GIS for flood modeling.

The present study has focused on exploring the applicability and usefulness of some of these advanced geo-spatial technologies in flood management by applying them in two flood prone river basins of Brahmaputra valley.

1.2. OBJECTIVES

The objective of this research is to study the following major components of flood risk reduction and potential for their application.

(a) Satellite based rainfall prediction using numerical weather prediction (NWP) techniques and its applicability for simple lumped and distributed hydrological models in basin scale.

(b) Applicability of satellite derived topographic datasets for extraction of river and floodplain configuration.

(c) To develop a multi criteria flood hazard assessment methodology using a combination of both remote sensing and field based parameters.

(d) Application of above three geospatial approaches in two major flood prone river basins at different altitudinal ranges of north bank of river Brahmaputra.

1.3. METHOD OF INVESTIGATION

In order to achieve the objectives of this research, the studies were carried out in different phases and are presented in the following chapters as summarized below:

To have state of the art knowledge on various topics relevant to this study, a detailed review of previous works done on different components of this research work has been carried out in a systematic manner and is presented in **chapter 2**.

In order to create a detailed knowledge base about various relevant characteristics of the two basins under study, existing departmental reports, field maps and other available documents etc have been referred to and valuable information relevant to the study area have been collected and are presented in **chapter 3**.

Synoptic weather monitoring with satellite based numerical weather prediction techniques provides an effective solution for rainfall forecast in absence of adequate surface observations. In **chapter 4**, scope and limitations of developing a moderately high resolution NWP model for a region having scanty data has been analyzed and applicability is validated by applying them in the study area.

Output generated from NWP models are used as main input to different hydrological models for prediction of flow leading to early warning for flood. Its applicability in a lumped model and a distributed models has been studied for both the river basins in **chapter 5**.

Accurate extraction of river channel and flood plain profiles plays an important role in river flood simulation studies. Satellite derived digital elevation data are most preferred choice of majority of researchers in this context. Although the global digital elevation model (DEM)s available freely in public domain such as SRTM, ASTER etc are popular choices among majority of the researchers, locally generated DEMs with photogrammetric techniques from satellite stereo data gives better surface representation especially in flat downstream floodplains.

A detailed comparison between a globally available DEM and a stereo DEM generated by photogrammetric techniques for extraction of river and floodplain profiles has been presented in **chapter 6**.

Effective regulation of human interference in floodplain also play important role in mitigating flood damages. For that, scientific delineation of different hazard and risk zones are important pre-requisites. A multi criteria remote sensing and field based flood hazard zonation technique has been developed for both the river basins. The high hazard zones thus obtained have been validated with inundation maps of real flood events of both the basins. The entire exercise has been presented in **chapter 7**.

Chapter 8 presents a comprehensive discussion of conclusion regarding applicability of all the geospatial approaches adopted in pursuit of achieving the major objectives of this study and their applicability for deriving hydro-morphological information for flood hazard management for other similarly situated tributaries of the Brahmaputra valley in particular and elsewhere in the world in general.

Chapter 2
LITERATURE REVIEW

2.1 INTRODUCTION

A brief review of previous landmark works done on various aspects of present research has been presented in this chapter. Past literatures that have been reviewed may be categorized as follows.

(i) Rainfall measurement and prediction techniques for forecasting flood

(ii) Different categories of rainfall-runoff models for prediction of flood

(iii) Use of topographic information for river channel and floodplain extraction

(iv) Flood hazard categorization techniques for flood risk mitigation

2.2 RAINFALL MEASUREMENTS

Rainfall is the most important meteorological parameter that influences the natural response of any river basins. Some prominent characteristics of any rainfall events are its intensity, duration and spatial distribution. Different approaches for rainfall measurements can be categorized as,

(i) Rainfall measurements by in-situ ground observations

(ii) Rainfall measurements through space based and other platforms

2.2.1 Rainfall measurements by in-situ ground observations

The most common precipitation measurement approaches under this category are Ordinary Rain Gauges (ORG), Automatic Rain Gauges (ARG), and Automatic Weather Stations (AWS) etc.

The ordinary rain gauge consists of a receptacle, a shell, a storage bottle, a storage vessel and a rain measuring glass which is a measuring cylinder graduated in precipitation amounts based on diameter of the receptacle's orifice. Rainwater entering through the receptacle accumulates in the storage bottle and precipitation amounts are measured with the measuring glass. The simplest form an ordinary rain gauge was developed by Richard Townley of United Kingdom in 1677. As reviewed by Middleton in 1953 the design standardization of ordinary rain gauges started in the late nineteenth century only. Figure 2.1 below shows the simplest

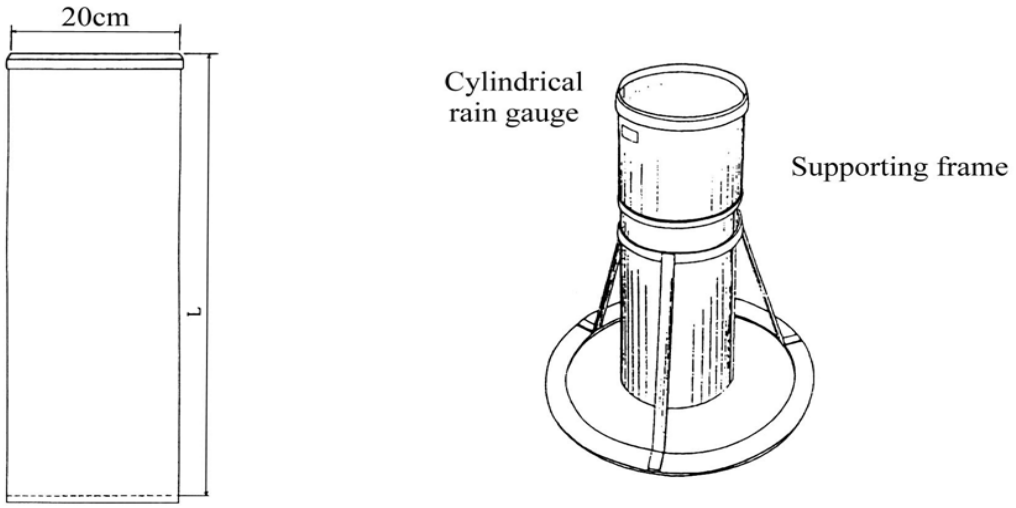

Fig. 2.1: The Line view (left) and the Solid view (right) of a simplest form of an ORG form of an ordinary rain gauge. The automatic or self-recording rain gauge consists of a rain water collector and a rainfall recording mechanism mounted on a base. The rainfall measuring unit consists of a float chamber containing a light metal float and a siphon chamber. The chart is wounded on a rotating drum driven by mechanical clock which rotates one revolution in 24 hours. The float rises along with rising water level and so is the recording pen thereby plotting a line on the chart. An Automatic Weather Station (AWS) typically consists of a weather proof enclosure containing the data logger, rechargeable battery, telemetry and meteorological sensor with an attached solar panel or wind turbine for its energy requirements. Apart from rainfall measurements, an AWS also measures other important meteorological parameters such as humidity, wind speed & direction, temperature etc. AWS plays important role in applications like real time rainfall runoff modelling, validation of rainfall forecast etc. Figure 2.2 below

Fig. 2.2: A typical AWS installed at a site under Brahmaputra valley

shows different component of an automatic weather station. As reviewed by Wood in 1946, the automation of rain gauges and weather stations was initially developed by the Radio section of the National Bureau of Standards, USA for the use of US Navy in 1939 and put on regular operational use in 1941. From then till date, the automatic rain gauges and weather stations have been technically improved many fold. Today a common AWS measures up to eight different weather parameters including rainfall, humidity, wind speed, wind direction, temperature, pressure, soil moisture etc.

Meteorological RADAR (Radio Detection And Ranging) in various forms has assisted weather predictions for over forty years but its operational use in hydrologic applications spans not more than a decade or so. The basics of radar based rainfall observation have been discussed by many authors (Battan 1973, Doviak and Jrinc 1993, Sauvageot 1991, Reinhart 1997). Figure 2.3 and 2.4 depicts the instrument flow, the data and a typical meteorological radar antenna. Radar based rainfall estimates use some algorithm to derive rainfall from the raw data that the instruments produce. The rainfall estimation techniques are being continuously improved and they provide varied accuracy that depends upon the season and

geographical location. However, the advantage of radar modes of data collection is the unparalleled spatial and temporal resolution. RADAR based rainfall estimation using next generation RADAR (NEXRAD) flood modelling has been discussed

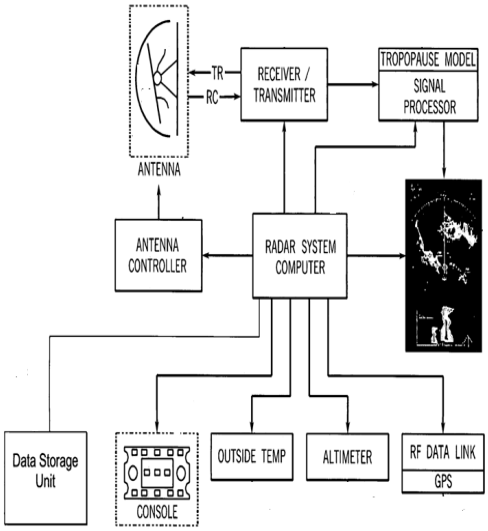

Fig. 2.3: Instrument flow of Met Radar
Source: DWR working manual

Fig. 2.4: A typical weather RADAR

in detail by Garrote and Bras, 1995 and Bedient *et al*. 2003. However there are other accuracy issues with RADAR measurement of rainfall such as location drift, time drift etc (Jayakrishnan *et al*. 2004) which limits the accuracy of flood forecast. In addition, the time required to convert the NEXRAD rainfall time series to a flood inundation map is critical in practical applications, especially during the extreme storm events that demand a highly efficient predicting capability.

Doppler weather radar (DWR), is a type of radar used to locate precipitation, calculate its motion, and estimate its type (rain, snow, hail etc.). Modern weather radars are mostly pulse-Doppler radars, capable of detecting the motion of rain droplets in addition to the intensity of the precipitation. Both types of data can be analyzed to determine the structure of storms and their potential to cause severe weather. Carlos *et al*. 2009 has presented a detailed comparison between radar rainfall and rain gauge data. Implications of uncertainty of radar based rainfall

measurements on hydrological model for flood prediction has been studies by Schroter *et al*. 2010.

2.2.2 Rainfall measurements from space based platform

Tropical Rainfall Measuring Mission (TRMM) is a joint space mission between NASA and Japan's National Space Development Agency designed to monitor and study tropical and subtropical precipitation and the associated release of energy. The mission uses 5 instruments: Precipitation Radar (PR), TRMM Microwave Imager (TMI), Visible Infrared Scanner (VIRS), Clouds & Earths Radiant Energy System (CERES) and Lightning Imaging Sensor (LSI). Many products on varying grids and temporal resolutions are available. The TMI is the main instrument used for precipitation measurements. Figure 2.5 below depicts a typical rainfall product from

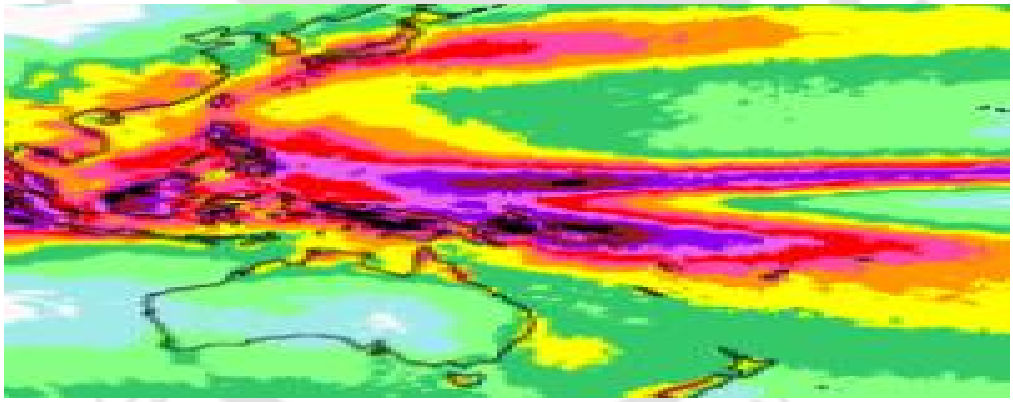

Fig. 2.5: TRMM rainfall measurement sample
(Source: trmm.gsfc.nasa.gov)

TRMM microwave imager. The key strength of TRMM products are high spatio-temporal resolution and updation at regular interval. The weakness is under estimation of precipitation at higher latitude regions.

2.3 RAINFALL PREDICTION TECHNIQUES

In order to achieve actionable lead time for flood prediction, rather than using measured in-situ rainfall through various means as mentioned in section 2.2,

predicted rainfall inputs are preferred for real time flood prediction with lumped and distributed hydrological model. Most promising among the prediction techniques are satellite based synoptic weather monitoring and the relatively recent Numerical Weather Prediction (NWP) models. Jain et al. 2001 have worked on influence of changing climate on flood.

2.3.1 Qualitative rainfall prediction by synoptic weather monitoring

In **satellite based synoptic weather monitoring**, mainly the cloud properties are studied by estimating the location, intensity, and duration of clouds over a particular area. This can be done with reasonable accuracy using satellite image in Thermal infrared (TIR, 10.5-12.5 μm wavelength range) band and Water vapour (WV, 5.7-7.1 μm) band. The data from both the channels should be studied in synchronization for better estimation of cloud properties over the area. Kalpana-1 satellite provides data in both the bands in 30 minutes interval. Figures 2.6. 2.7 and 2.8 below depicts satellite

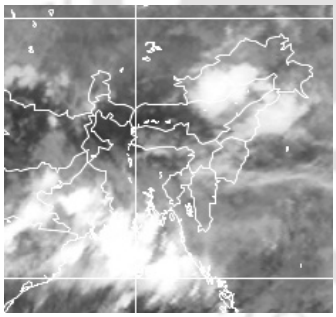

Fig. 2.6: Visual channel

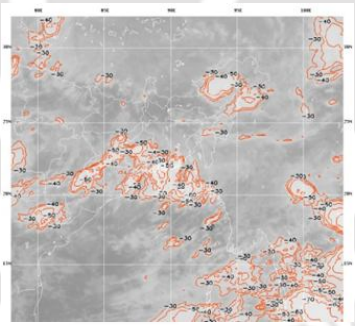

Fig. 2.7: TIR Channel

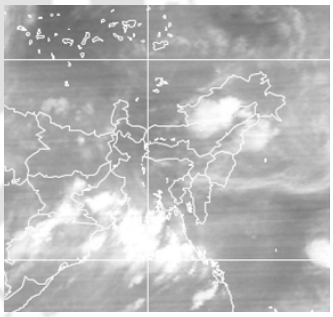

Fig. 2.8: WV channel

(Source: imd.gov.in)

based cloud data of the north eastern region of India in Visual, Thermal Infra-red (TIR) and Water vapour (WV) channel (Source: India Meteorological Department web portal).

The cloud motion vector (CMV) is available from a lot of sources like IMD, MOSDAC, CIMSS (USA), etc. It is available for lower level atmosphere and upper

level atmosphere separately. The CMV provides speed and direction of cloud and thus of wind at different pressure level. This information helps in deciding whether a particular system (of cloud) within certain interval of time, will arrive over the area of concern or go away from it. Such diagnosis helps in forecasting synoptic weather scenario during night time, when real time observation is not done. Figures 2.9 and 2.10 below depict CMV data of upper and lower atmosphere (data sources: CIMSS, Wisconsin University, USA).

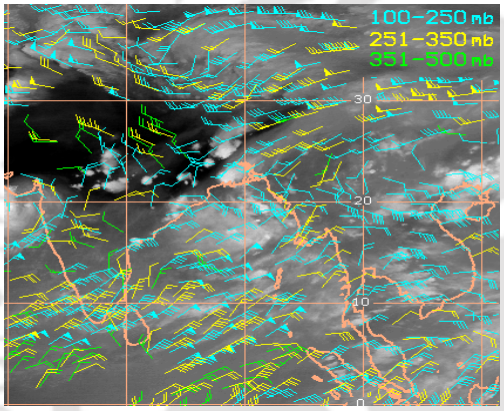

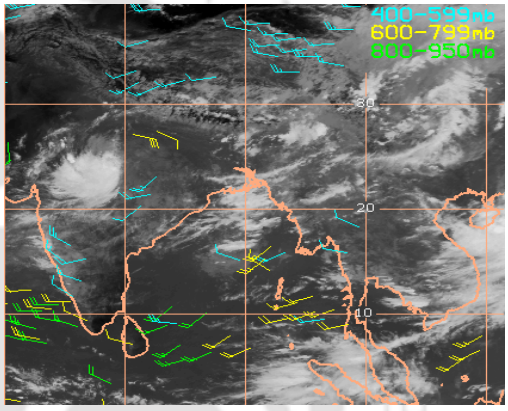

Fig. 2.9: CMV of upper atmosphere Fig. 2.10: CMV of lower atmosphere
(Source: imd.gov.in)

The **atmospheric vorticity** is computed using finite difference approximation of first derivative of v and u with respect to x and y respectively, where u and v are the wind components east-west and north-south directions respectively and x and y are the horizontal grid spacing (spatial resolution of u and v). u and v are obtained from gridded atmospheric motion vector (AMV) products prepared from satellite data. These u and v are computed for different atmospheric pressure level. One of the readily available product is 850 mb vorticity, generated using u and v at 850 mb pressure level. Physically vorticity is a measure of curvature in atmospheric flow. A positive value indicates clockwise motion in the northern hemisphere and

counter clockwise motion in the southern hemisphere. A positive vorticity environment, indicating upward air flow, is conducive to storm development, while negative vorticity indicated downward air flow indicating subsidence of air over the place, thereby suppressing convection. Figure 2.11 below shows a moderate to strong vorticity over the Indian Sub-continent which is indicative of development of rain bearing clouds over different regions in coming 12 to 24 hours.

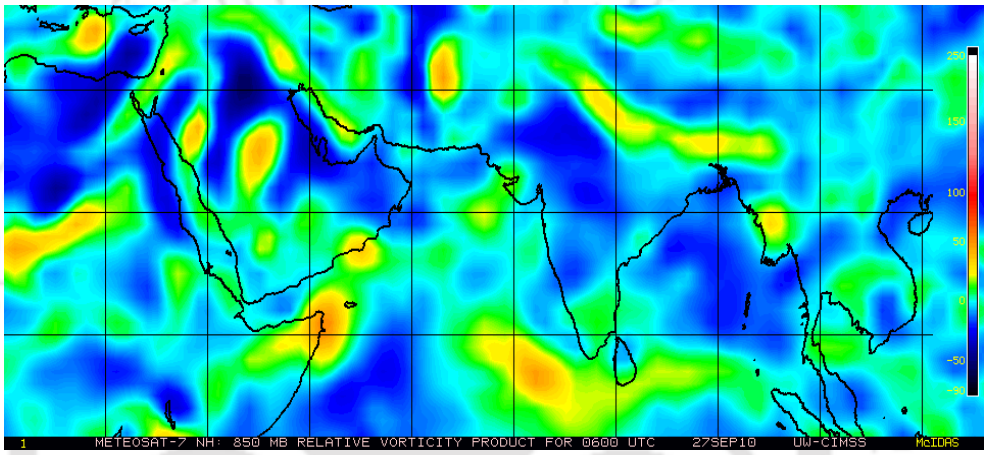

Fig. 2.11: Atmospheric vorticity data over Indian sub-continent
(Source: Wisconsin University, USA)

2.3.2 Quantitative rainfall forecasting by Numerical Weather Prediction (NWP)

Recent advances in technology have enabled rainfall forecast and estimations through various other means. Most promising among them are the rainfall forecast from Numerical Weather Prediction (NWP) models. NWP is the science of predicting the weather using models of the atmosphere and computational techniques. There are a number of NWP model to forecast meso-scale weather system. As reviewed by Frederick G Shuman in 1978, the idea of numerical weather prediction was first recorded in paper by Vilhelm Bjerknes in 1904 where he discussed the applicability of physical laws for predicting the

atmosphere. More than a decade later, Lewis Fry Richardson in 1922 gave a detailed description of the tasks required to acquire and process data and finally disseminate forecasts. The most basic problem at that time was the gross inadequacy of computational facilities. With the advent of electronic computers from 1940 onward, the first operationally robust NWP model was developed by Jule G Charney in 1949 which was further improved computationally by Goldstine in 1972. From then till early twenty first century, many researchers have contributed towards the development of numerical weather prediction model as an effective tool for weather prediction in general and rainfall prediction in particular. There are a number of NWP model to forecast mesoscale weather system. Prominent among them are MM5, ARPS, WRF etc.

The **MM5 model** is a non hydrostatic primitive equation model, with versatility to choose the domain region of interest; horizontal resolution; interacting nested domains and with various options to choose parameterization schemes for convection, planetary boundary layer, explicit moisture, radiation and soil processes. This NWP model has been developed from a mesoscale model used by Anthes at Penn State in the early 70's that was later documented by Anthes and Warner in 1978. Since that time, it has undergone many changes designed to broaden its usage. The model can be designed to have number of interactive nested domains with horizontal resolutions such as 36, 12 and 4 km etc. The model is supported by several pre- and post-processing programs, which are referred to collectively as the MM5 (Meso-scale Model 5) modelling system. The MM5 modelling system software is mostly written in FORTRAN, and has been developed at Penn State and NCAR as a community meso-scale model with contributions from users worldwide. Terrestrial and isobaric meteorological data

are horizontally interpolated (programs TERRAIN and REGRID) from a latitude-longitude mesh to a variable high-resolution domain on a Mercator, Lambert conformal, or polar stereographic projection. Since MM5 is a regional model, it requires an initial condition as well as lateral boundary condition to run. To produce lateral boundary condition for a model run, one needs gridded data to cover the entire time period for which the model is integrated. Yamazaki *et al*. 2005 have worked for mesoscale precipitation forecasting using MM5 model for a region over Portugal. Similarly Akter *et al*. 2007 has worked for rainfall forecasting over region of Bangladesh using coarse resolution grid of the order of 45 km with MM5.

The **Advanced Regional Prediction System (ARPS)** model was developed by the Centre for analysis and prediction of storms, University of Oklahoma in 1989. Its formal mission was to demonstrate the practicability of storm-scale numerical weather prediction and to develop, test, and validate a regional forecast system appropriate for operational, commercial, and research applications. Its ultimate vision was to make available a fully functioning storm-scale NWP system as mentioned by Lilly in 1983 and Droegemeier in 1997. The numerical prediction component of the ARPS is a three-dimensional, non-hydrostatic compressible model formulated in generalized terrain-following coordinates. It is designed from the beginning to run on computing platforms ranging from single-processor scalar workstations to massively parallel scalar or vector processors. The ARPS contains a comprehensive physics package and a self-contained data analysis, radar data retrieval and assimilation system. It has been subjected to real-time weather prediction testing over several regions since mid-90s by researchers like Droegemeier *et al*. 1996; Xue *et al*. 1996; Carpenter *et al*. 1999 and Shin *et al*.

1998. As cited by Xue *et al*. 2002, during spring of 1998, ARPS participated in a unique multi-model mesoscale ensemble prediction experiment.

Weather Research and Forecasting (WRF) model is another such technique which is extensively used worldwide due to their highly developed physics schemes and better time integration method to give improved forecast at shorter duration. It also includes a data Assimilation module called Weather Research Forecast Data Assimilation (WRFDA) where observed data can be fed to update the model's initial condition to generate realistic forecast. This model has been developed out of a multi-agency collaborative effort during early nineties. This group of agencies consists of National Centre for Atmospheric Research's (NCAR) Mesoscale and Micro scale Meteorology (MMM) Division, the National Oceanic and Atmospheric Administration's (NOAA), National Center for Environmental Prediction (NCEP) and Earth System Research Laboratory (ESRL), the Department of Defence's Air Force Weather Agency (AFWA) and Naval Research Laboratory (NRL), the Centre for Analysis and Prediction of Storms (CAPS) at the University of Oklahoma, and the Federal Aviation Administration (FAA) of US. The strength and limitations of this model have been studied by my many researchers in recent times.

Wardah *et al.* 2011 has described a comparison between the MM5 and WRF model for a tropical river basin in Malaysia. They have opined that both the models perform relatively better in case low rainfall than in case of heavy rainfall.

Raje and Mujumdar in 2011 have worked significantly on comparison of down scaling methods for daily precipitation.

Sammany *et al.* 2010 has also presented a case study on the usefulness of WRF derived rainfall forecast for forecasting a flash flood event. He has

successfully reproduced a rainfall forecast leading to a flash flood event with a reasonably good lead time.

Maussion *et al.* 2011 have tried a comparison of performance between TRMM rainfall data with that of WRF derived rainfall over Tibetan Plateau when separately compared to surface observations.

2.4 HYDROLOGICAL RAINFALL RUNOFF MODELS FOR FLOOD PREDICTION

The hydrological behaviour of a catchment depends on storm characteristics (Intensity, duration and spatiotemporal distribution) as well as static catchment characteristics such as area, slope, shape, land-use and soil type. Many hydrological models are available for modelling rainfall run-off of a watershed for computing an upcoming discharge in order predict a possible flood situation. The history of scientific rainfall-runoff modelling begun about 3 centuries ago with the report on quantitative measurements in hydrology published by P. Perreaultin 1674 which has been reported by Mishra and Singh in 2003. By comparing the measured annual rainfall (Pa) and the estimated annual stream flow (Qa) of the Seine river near Paris, Perreault described a functional relationship as Qa= Pa/6. In the context of modern hydrology, the development of this Pa-Qa relationship is very primitive, but it was a major finding of the time. It is worth noting that concept of computing runoff as a percentage of rainfall is still in use after 325 years according to Mishra and Singh in 2003.

2.4.1 Lumped models for run-off computations

The most well known models for rainfall runoff modelling are the Rational

method, the unit hydrograph method and the SCS-CN method.

Rational method for estimating the peak discharge from small urban and rural watershed as cited by Viessman and Lewis in 2008 was introduced in US by Emil Kuichling in 1889. This method is traditionally used to size storm sewer, channel and other drainage structures. Rational method assumes that rainfall duration equals to the time of concentration which results in the greatest peak runoff. According to Zoppou in 2001 and Hayes and Young in 2006 the rational method has wide applicability due to its simplicity. Rational method assumes a factor to consider all the losses while calculating runoff (infiltration, evaporation, transpiration, initial abstraction and depression storage). This factor is called runoff coefficient (C) and the value of C is determined by observation and experience.

The Rational formula is

$$Q = 0.0028\ C\ I\ A \qquad (2.1)$$

Where,

Q = Peak rate of runoff (Cumec)

I = Maximum rainfall intensity (mm/hr) for a duration equal to the time of concentration for the designed frequency

C = Runoff coefficient

A = Area (Ha)

Limitation of the Rational method is that it provides only the peak discharge from a watershed, not a complete hydrograph, and therefore it cannot be used for routing multiple flows toward a single outlet. However, for a quick approximate assessment of the magnitude of a probable upcoming flood

discharge, rational formula is useful.

Sherman in 1932 first developed the concept of Unit hydrograph. Many researchers have defined the same concept with different analogies. The unit hydrograph is a hydrograph that results from unit excess rainfall (1 inch or 1 mm) uniformly over a watershed during a given period of time.

As studied by Cavallini in 1993, the unit hydrograph method has the advantage of providing a complete storm hydrograph for describing the rainfall runoff relationship. While dealing with complex watersheds, the storm hydrograph for each sub watershed can be computed independently by the unit hydrograph method for subsequent routing down the main channel. However, the chief weakness of this method is involving the determination of infiltration loss. Various other methods that are based on the concept of Unit Hydrograph are also developed by different investigators to study rainfall runoff behaviour. Agirre *et al.* 2005 proposed the Geomorphologic Unit Hydrograph of Reservoirs (GUHR) and compared the model with Nash's Instantaneous Unit Hydrograph (Nash's IUH) while applying it to Aixola watershed of Northern Spain. Both the models showed similar behaviour, however GUHR was more preferred for considering the watershed morphology.

The **SCS-CN model** for small watersheds has been used extensively. The SCS-CN (or curve number method) was developed by the USDA Natural Resources Conservation Service (SCS, 1956). This is an empirical method and widely used for determining the approximate amount of direct runoff from a rainfall event in a particular area. The runoff curve number is based on the area's hydrologic soil group, land use, treatment and hydrologic condition.

The popular form of SCS – CN method is

$$Q = \frac{(P - I_a)^2}{P - I_a + S}$$

(2.2)

Where,

Q is runoff ([L] ; In)

P is rainfall ([L] ; In)

S is the potential maximum soil moisture retention after runoff begins ([L]; in)

Ia is the initial abstraction ([L]; in), or the amount of water before runoff, such as infiltration, or rainfall interception by vegetation; and it is generally assumed that $I_a = 0.2S$

In the Curve Number method, S and CN are related as

$$S = \frac{1000}{CN} - 10 \qquad (2.3)$$

CN has a range from 30 to 100; lower numbers indicate low runoff potential while larger numbers are for increasing runoff potential. The lower curve number indicates more permeable soil condition.

Mack in 1995 developed an interactive computer model called HER (Hydrological Evaluation of Runoff) with the SCS-CN method. Patil *et al.* 2008, while indicating the natural resources conservation services curve number (NRCS-CN) method as one of the most widely used methods for quick and accurate estimation of surface runoff from ungauged watersheds, developed an ArcGIS interface to estimate the surface runoff by adopting the

NRCS-CN technique and its three modifications. The developed interface was validated using the recorded data for the periods from 1993 to 2001 of a gauged watershed, Banha, in the Upper Damodar Valley, Jharkhand, India and concluded that the application of the modified CN- I method in the ungauged watersheds that are hydrologically similar to the Banha watershed would result in an accurate surface runoff estimation. Shi *et al*. 2009 determined the initial abstraction ratio (Ia) in an experimental watershed in the Three Gorges Area of China, by analyzing measured rainfall-runoff events and compared the performance of the traditional and modified ratio of initial abstraction (Ia) to maximum potential retention (S) with observed rainfall-runoff data. This Ia/S-adjusted SCS-CN method appears to be better for runoff prediction in the three Gorges Area of China.

CN numbers are now available for different land uses. Its limitation is that it does not provide the peak flow directly. However some relationships are now developed that can convert run-off volume into peak flow.

2.4.1 Distributed models for run-off computations

Distributed hydrologic models, with the capability to incorporate a variety of spatially-varying land characteristics and precipitation forcing data, are thought to have great potential for improving hydrologic forecasting. Distributed models use parameters which are directly related to the physical characteristics of a watershed. These include topography, soil, vegetation etc. Distributed models also account for the spatial variability of the meteorological conditions of the drainage basin as opined by Refsgaard in 1997 and Schulz in 2006.

The **Variable Infiltration Capacity (VIC)** model developed by Liang *et al*. during 1994 to 1996 is a spatially distributed hydrologic model that solves the water

balance at each model grid cell. It incorporates spatially distributed parameters describing topography, soils, landuse, and vegetation classes. VIC is considered a macro-scale hydrologic model which is designed for larger basins with fairly coarse grids. In this manner, it accepts input meteorological data directly from global or national gridded databases or from GCM projections. To compensate for the coarseness of the discretization, VIC is unique in its incorporation of sub-grid variability to describe variations in the land parameters as well as precipitation distribution. Parameterization within VIC is performed primarily through adjustments to parameters describing the rates of infiltration and base flow as a function of soil properties as well as the soil layer's depths. Bao *et al*. 2011 have used the variable infiltration capacity model for river base flow computation in un-gauged basin.

The **TOPMODEL** developed by Bevan and Kirkby in 1979 is a versatile hydrological model at catchment scale based on a simple topographic description and runoff mechanisms including both saturation excess and infiltration excess runoff. The model is very sensitive to changes of the soil hydraulic conductivity decay parameter, the soil transmissivity at saturation, the root zone storage capacity and the channel routing velocity in larger catchments. As studied by Franchini *et al*. 1996 and Saulnier *et al*. 1997, the calibrated values of parameters are also related to the grid size used in the digital terrain analysis. The time step and the grid size have also been found to influence the TOPMODEL simulations by Bruneau *et al*. 1995. Overall, TOPMODEL is a simple and versatile model whose major advantages are its parametric parsimony and the capability to visualise the simulation results in a spatial context.

The **TIN-based Real-Time Integrated Basin Simulator (tRIBS)** is a physically-based, distributed hydrologic model developed at the Ralph M. Parsons Laboratory, Massachusetts Institute of Technology. The model emphasizes the dynamic relationship between a partially saturated zone and the land surface response to the continuous storm and interstorm cycle. This is performed by tracking the evolution of moisture fronts within a computational element in relation to the water table depth position. One-dimensional infiltration in the surface normal direction is redistributed by both the lateral fluxes in the zone and in the phreatic aquifer during storm and interstorm periods. By modelling these detailed processes, tRIBS is capable of producing runoff through a number of generation mechanisms including infiltration-excess, saturation from below and perched saturation-excess runoff. In combination, these processes allow tRIBS to model the development of partial contributing areas within the basin. Currently, the runoff produced from these areas is routed to the outlet using a simplified scheme that allows non-linearity in the routing through the channel network. A set of Matlab scripts is available for the application of the Shuffled Complex Evolution (SCE) algorithm developed by Duan *et al.* 1993 for parameter optimization and calibration in the tRIBS model.

The **Soil & Water Assessment Tool (SWAT)** is a public domain model jointly developed by USDA Agricultural Research Services (USDA-ARS) and Texas A & M University in US in 1990. SWAT is a small watershed to river basin scale model to simulate the quality and quantity of surface and ground water. Jha *et al*. 2004 have used SWAT based flow simulation for appropriate division of watershed into sub-watersheds. Gosain *et al.* 2005 have used SWAT for return flow computation in irrigation command area.

The **Hydrologic Engineering Centre's Hydrological modelling System (HEC-HMS)** is a rainfall-runoff model developed by the US Army CORPS of Engineers (USACE-HEC) in 1998. It utilizes a graphical interface to build a semi distributed watershed model in order to set up rainfall and control variable for runoff simulation. HEC-HMS allows the modeller to choose between numerous infiltration loss parameterizations (HEC, 2000). However, only the gridded curve number (CN) technique enables spatially distributed infiltration calculations. Infiltration capacity is quantified in a parameter derived by the Soil Conservation Service (SCS) called the CN. The CN is a method for determining storm runoff over an area based on land use, soil and land cover type, and hydrologic soil group (USSCS, 1986). Soil groups are determined based on type and infiltrability of a soil. Here the infiltration loss is derived by none other than the widely used SCS Curve Number (Equation 2.2 and 2.3 above) method. The development of the flood model integrates GIS with the HEC-HMS rainfall runoff model. Numerous past studies have shown these models to provide accurate and useful results in flood related studies. Prominent among them were carried out by Ahrens and Maidment in 1999 and Anderson *et al*. 2002. Of late Kashid and Gupta in 2010 have used both HEC-HMS and HEC-RAS for hydrologic and hydraulic modelling respectively. The present research work also focuses on the usefulness of HEC-HMS model with input from rainfall predicted through Numerical Weather Prediction models for prediction of flood discharge in watershed scale.

2.5 USE OF TOPOGRAPHIC INFORMATION FOR RIVER CHANNEL AND FLOOD PLAIN STUDIES

Topographic information plays important role for different basin scale flood management studies such as flood inundation modelling, flood hazard zonation,

river channel routing, hydro-meteorological flood discharge prediction etc. There are different ways of extracting topographic information of a river basin. Johnson and Padmanabhan in 2010 have worked on importance of river geometry for estimation of design flows at ungauged sites.

2.5.1 Sources of topographic Information

Contour survey data is the most primitive form of topographic information for various types of flood related studies. It is also one of the most precise topographical information so far as vertical accuracy is concerned. Starting from simple levelling instruments like the dumpy level, contour survey has come a long way through instruments like the Theodolite and more recent addition are the present day modern total stations. In spite of being precise, this form of survey is generally not preferred because of its slow and tedious procedure. It takes long time to cover relatively small area. Finer the contour interval, more tedious and time consuming the survey is. The most widely used Survey of India (SOI) reference maps in 1:50,000 and 1:2,50,000 scale is one of the largest exercise in topographical survey history.

Topographic data acquisition from remote sensors started with aerial photography from airborne platforms such as hot air balloons, low flying gliders, small aircraft etc. That was the beginning of stereo photogrammetric techniques for extraction of topographic maps. Later on raster based digital elevation data started getting generated, and because of their spatial compatibility with different regional and global co-ordinate systems, Digital Elevation Model (DEM) as it is known now, has become the most widely used elevation information for all types of scientific studies involving the undulation of the earth surface including river channel and

flood plain studies. In recent years there has been tremendous development of new technologies for extraction of topographic elevation information. Some of these technologies worth mentioning are Satellite stereo photogrammetry, Synthetic Aperture Radar (SAR) interferometry, differential SAR interferometry and the most modern Light Detection and Ranging (LiDAR) based topographic mapping.

2.5.2 Globally available coarse Digital Elevation Models

Because of the world wide demand for digital elevation data among researchers and scientists for various scientific and engineering applications, different space agencies have made their Digital Elevation Models available freely in the public domain for the benefit of scientists and science. Although these DEMs are generally of coarse spatial resolution, still scientific community have been greatly benefitted by availing these freely available global DEMs. Some of the widely used global DEMs are discussed here with special emphasis on their applications in flood plain related studies.

The Shuttle Radar Topography Mission (SRTM) digital elevation model (DEM) produced originally by NASA is a major breakthrough in digital mapping of the earth surface as cited by Van in 2001 and provides a major advancement in the accessibility of high quality elevation data for researchers worldwide. The SRTM data is available as 3 arc second (approx. 90m resolution) DEMs. A 1 arc second data product was also produced, but is not available for all countries. The vertical error of the DEM's is reported to be less than 16m. The data currently being distributed by NASA/USGS in public domain. Sanders in 2007 has evaluated the capability of SRTM DEM for flood inundation modelling. He has also compared it with other freely available online DEM for the purpose of flood plain inundation

simulation. Vertical precision has been found to be lacking due speckle or noise as demonstrated by Sanders in 2007. However the vertical accuracy of the SRTM can be improved by about 40% by incorporating ground control points (GCP) with the help of GPS as demonstrated by Gorochovich *et al*. 2006.

The Advanced Space borne Thermal Emission and Reflection (ASTER) digital elevation model is another globally available elevation data with a spatial resolution of 30m. ASTER GDEM is an easy-to-use, relatively accurate DEM covering all the land on earth, and available to all users regardless of size or location of their target areas. Pre-production estimated accuracies for this global product were 20 meters at 90 % confidence for vertical data and 30 meters at 95 % confidence for horizontal data (as per developer's home page).

Falorni *et al*. 2005 characterized and analysed the vertical accuracy aspect of the DEM from SRTM. He found the drawback of radar based DEMs like speckle, or random noise, which degrades relative vertical accuracy particularly on floodplains. Comparison between SRTM and ASTER has not been brought to focus under the present research work due to the difference of their origin of as SRTM is a radar based DEM where as ASTER is based on thermal emission.

Gichamo *et al*. 2012 has studied about the capability of ASTER DEM for extraction of river geometry in stable river mostly with clear water at Hungary with encouraging results. As the same needs to be examined for fragile alluvial sediment laden rivers as that of Brahmaputra valley, ASTER has been taken as the global course DEM for its comparison with a local finer DEM for extraction of river cross sections as part of the present research work.

2.5.3 Locally generated moderate and fine resolution Digital Elevation models

Depending on the accuracy and precision requirements, sometimes globally available DEMs become inadequate for extracting earth surface with desired accuracy. In those situations, digital photogrammetry plays important role. Several techniques are found to be suitable for DEM extraction like digital aerial and terrestrial photogrammetry, airborne and terrestrial laser scanning, GPS methodology with its different measurement approaches and active and passive remote sensing, with optical satellite imagery systems (Fraser *et al*. 2002). For most hydrological applications, the vertical resolution of a DEM is considered satisfactory when the ratio of the average drop per pixel and the vertical resolution is more than unity (Theiken *et al*. 1999).

DEMs can be generated by traditional photogrammetry based on aerial photos if they are available and not classified, but also very often more economic by means of satellite images. As studied by Jacobsen in 2001, the achieved accuracy of DEMs based on satellite images is mainly dependent upon the image resolution, the height-to-base-relation and the image contrast. In addition, systematic image errors of photographic products and limited orientation quality may cause a difference between relative and absolute accuracy.

SPOT images were one of the first pairs of stereo images for generation of DEMs by digital photogrammetry. Similarly other stereo pairs such as IRS-1C/1D, TK 350 etc have been used for creating moderate resolution DEM with vertical precision of around 5 to 10 meters which were found to be not adequate enough for river and floodplain studies. Then few years back the high resolution stereo pairs like the IKONOS, CORONA and QUICKBIRD etc were found by number of researchers to be more suitable for hydrological applications. One such high resolution DEM can be generated from the stereo pairs of CARTOSAT – I (IRS

P5) satellite launched by the Indian space agency ISRO. Krishna Murthy *et al*. 2008 have studied the various processing details of the CARTOSAT – I stereo photogrammetry for creation of CARTOSAT – I DEM. They have also compared its planimetric and vertical accuracy with respect to other high resolution reference DEMs.

Obstruction created by cloud cover in optical data, often adversely affects the vertical continuity of the generated DEM and therefore image recorded during cloudy day are found to be unfit for generation of DEM. With the launch of recent Synthetic Aperture Radar (SAR) satellites such as Terra- SAR X, RADARSAT-2 etc, have paved the way for generation of DEM with high vertical accuracy and seamless continuity as opined by Xu *et al*. 2011.

Light Detection and Ranging (LiDAR) is the most up to-date technology for generation of precise and accurate DEM. Airborne LiDAR sensors emits between 5000 to 50,000 laser pulses in a scanning array. Each laser pulse has a pulse width between 0.5 m to 1 m. Both vertical and horizontal accuracy of LiDAR DEM largely depend on this pulse width. LiDAR is better able to map the bare earth elevations by penetrating through forested and other vegetated earth surfaces. The post spacing of LiDAR DEM is considerably denser than that of other DEMs making it more suitable for mapping minute vertical undulations of gentle floodplain topography. However a major disadvantage of LiDAR is that the contours derived from it are normally not hydro corrected which is important for ensuring the downward flow of water in the DEM. Aguilar *et al*. 2010 have presented the applicability of LiDAR DEM for detection of lateral movement river bed. Although LiDAR survey has conclusively been proven to be useful for hydro

morphological mapping, the products are still not affordable and processes like data filtering for noise removal etc are also tedious.

2.5.4 Applicability and limitations of different DEMs for extraction of floodplain features

River geometric data (both cross section and longitudinal profile) is the most vital input for hydraulic modelling of flood plain and accurate extraction of this geometry is the key to the success of any river modelling exercise as opined by Bloschl *et al*. 1995. After the advent of Remote Sensing and GIS technology, hydrographical surveys have been mostly replaced by various satellite images and radar based Digital Elevation Models for generation of river geometry for flood modelling exercise. However based on the horizontal and vertical resolutions of different DEMs, there are merits and demerits of these DEMs for different types of flood plain studies.

In recent years, there has been an increasing move toward using automated digital correlation techniques to generate what are known as "photogrammetric DEMs" directly from stereoscopic imagery, especially where contour data are not available or are not accurate enough as opined by Robinson in 1994. Few studies have been undertaken on the effects of relative elevation accuracy in published DEMs on hydrologic modelling or geomorphic parameters used in hydrology. Zhang and Montgomery, in 1994 and Wolock and Price, 1994 have investigated the effect of grid size on the topographic index.

Regarding applicability of the ASTER DEM for extraction of flood plain geomorphic features, Kamp *et al*. 2003, concluded its suitability for extracting macro and meso-relief for stable flood plains of Germany but also about its limitations for extracting micro relief.

Sanders, 2007 carried out a detailed comparison of coarse resolution online DEMs with photogrammetrically generated moderate and fine resolution DEMs for extractions of flood plain features required for inundation modelling. In his paper he has concluded the inapplicability of both 90m and 30m SRTM DEMs for extraction floodplain features due to data gaps such as radar speckle and radar shadow. He further concluded that other DEMs such as National Elevation Dataset (NED) , NOAA IfSAR etc, inspite of having good horizontal resolution, are incapable of representing the bare earth elevations due to not being able to penetrate below the vegetated, forested floodplain topography. In his conclusion the DEMs derived from airborne LIDAR has been opined to be the most suitable for extracting river geometry for flood modelling due to its capability of accurately extracting the bare earth elevations irrespective of the overlying vegetation cover. Further Wang *et al*. 2012 have opined the acceptance of ASTER, SRTM etc in higher altitude only in absence high resolution stereo graphic DEMs. But whether the same opinion holds good for flood plains of lower altitude such as that of the Brahmaputra valley needs to be examined and it has been tried in the present research work.

2.6 FLOOD HAZARD ZONATION TECHNIQUES

Seasonal river flooding is an inevitable natural phenomenon occurring time to time in almost all drainage systems in the world during heavy precipitation in their respective watersheds. It is a natural process of formation of river morphology that sometimes the river needs to overflow its own defined channel. With the development of human civilization, anthropogenic interventions on the flood plain and lower terrace areas of rivers have significantly increased. Thus due to gradual encroachment of the natural flood plains by human population for Agriculture and

other livelihood purposes, the earlier simple flooding phenomenon has now become a recognisable disaster creating severely adverse impact on human lives and property. Hence it has been thought about by both the socio-economic and scientific communities to regulate flood plain usage in order to minimize damages to life and property. Identification of flood prone areas with different degrees of associated hazard (the probability of occurrence of a potentially damaging phenomenon as stated by Varnes in 1984) or flood hazard zonation is a vital input for scientific management of flood hazard and to mitigate flood damages. In comparison to other hydrological studies related to flood plain, hazard zonation is relatively new research area. From the techniques that have been developed till date, three prime approaches of flood hazard zonation can be categorized. They are (a) Zonation based on existing historical records, (b) Zonation based on flood inundation modelling and (c) Zonation based on multi-criteria hazard evaluation.

2.6.1 Flood hazard zonation by occurred inundation records

In many countries, stream-gauging records are insufficient or absent. As a result, flood hazard assessments based on direct measurements may not be possible, because there is no basis to determine the specific flood levels and recurrence intervals for given events. Hazard assessments based on remote sensing data, damage reports, and field observations can substitute when quantitative data are scarce. They present mapped information defining flood-prone areas which will probably be inundated by a flood of a specified interval (Riggs, 1985). Simplest form of flood hazard categorization is by analysing a time series of historical inundation maps in GIS platform. Chen, 1999 and Mongkolsawat, 2003 both have studied the applicability of RADARSAT SAR data in GIS domain for flood hazard zonation. The extent of flood inundation is extracted from the satellite data and

flood maps at various scales i.e. state, district and detailed levels are prepared for the flood affected states in India (Bhatt *et al*. 2011). A time series of these yearly flood inundation maps have been overlapped in GIS platform to prepare flood hazard zonation maps. The degree of hazard has been determined based on number of times a particular area has been inundated over the period of time series data. Apart from being the simplest, the hazard zones created this way also serves as validation ground data for hazard zones categorized by other approaches of flood hazard zonation. The present research work has also used such hazard zonation maps for validation of hazard zones created by other approaches. One of the advantages of this approach is that even old historical flood inundation maps can also be scanned and brought to GIS platform by proper geo-rectification and may be used in combination with satellite derived inundation maps for the analysis of flood hazard. In this approach the scale of the hazard zonation is dependent on the scales of input inundation maps. A disadvantage of this hazard zonation approach is that it is dependent on availability of inundation records and sometimes excludes even highly potential flood prone areas due to missing inundation records. Longer the time series of inundation records better is the flood prone area delineation and categorization with approach.

2.6.2 Flood hazard zonation by flood inundation modelling based on flood frequency

Flood inundation models combined with Digital Terrain Models, describe the processes taking place in the flood plain, and have shown significant progress in latest years. The basis for flood inundation models is a Digital Terrain Map (DTM) of the flood plain area (Integrated flood risk analysis and management methodologies, http://floodsite.net). Digital Terrain Maps are often produced

based on ground survey data, optical stereo images, Radar images and laser scan data. Empirical methods are often described as pure mapping. No physical laws are involved in the simulations performed. They are rather simple methods compared to the others, with low cost, but they provide poor estimates of flood risk in large low lying or extensive areas where flows through a breach may be critical in determining the flood extent. They are usually applied to assess flood extents and flood depths in broad scale. Arc-GIS and Delta mapper are example models which usually describe flow processes in compound channels. These models use Digital Elevation Models (DEM), upstream water level and downstream water level as inputs and calculate inundation extent and water depth by intersecting planar water surface with Digital Elevation Maps. The computational time is less in these processes.

The evaluation of flood risk is very complex due to uncertainties of the problem and the oversight of observed data, especially for high return period discharges. This problem it is more difficult to solve in very flat areas because of the small changes in the land surface elevation models (Sole *et al*. 2008). The topographic data resolution affects the accuracy of the overland flow routing in flood inundation modelling.

Horritt *et al*. 2001 has studied the affect of spatial resolution on raster based flood models. He has experimented with a finite element hydraulic model aiming to solve the shallow water equations for inundation modelling.

Dyhouse *et al*. 2005 has worked on applicability of HEC-RAS for flood plain modelling as it estimated hydraulic profile for gradually varying flow in natural and artificial channel. Sarma *et al*. 2001 has also worked extensively on simulation of gradually varied flood wave propagation due to dike failure.

MIKE 21 is a 2D free surface flow model developed by the Danish Hydrologic Institute. This model has been extensively used for flood plain inundation modelling for flood frequency based hazard zonation.

2.6.3 Flood hazard zonation by multiple criteria

As discussed in previous sections , both flood hazard zoning by historical inundation records as well as flood inundation simulation models have some limitations and shortfalls which have prompted researchers to work with other methods for classification of flood hazard. Flood hazard zoning by multi criteria weight assignment and ranking has been a relatively new area of research in flood hazard categorization. River basin and flood plain geo-morphology plays important role in this aspect. Woolman in 1971 has demonstrated the effectiveness and appropriateness of geo-morphologic method and it was supported by Lastra *et al*. 2008 with the application of aerial photographs in combination with field investigation of flood evidences.

A geomorphologic map can help to study the extent of inundation area, direction of flood flows, and changes in river channel through remaining flood evidences, relief features and sediment deposits formed by repeated flood, hence understanding the nature of former flood and probable characteristics of flood occurring in the future as opined by Oya, 2002. This approach of flood investigation has been verified significantly by Lastra *et al*. 2008 where the channel system and floodplain morphology of rivers change dynamically and have high erosive potential and substantial sediment supply.

The use of spectral indices and band ratios for discriminating flooded area and non flooded area has been initially attempted by Wang *et al*. 2002 with the LANDSAT TM data.

Sinha *et al*. 2008 attempted a multi-parametric approach using analytical hierarchy for generating a flood risk index (FRI) in Kosi river basin where proximity to active channel has been used as one of the parameter.

Ho *et al.* 2010 have attempted the usefulness of Normalised Difference Water Index with LANDSAT TM data for distinguishing between flooded areas and dry lands.

2.7 IN CONCLUSION OF LITERATURE REVIEW

Existing literatures related to different approaches for derivation of hydro-morphological input for management of few vital aspects of flood hazard have been reviewed. Following scenarios have emerged for further studies.

In the area of use of non conventional sources of rainfall input for running hydrological run-off models as required for flood forecasting, synoptic rainfall measurements using weather RADAR has been widely used all over the world. There also locally installed radars have been found to perform better than global RADAR on satellite based platforms. As RADAR outputs are also real time measurements, hence have not proven to be of much usefulness so far as increasing the forecast lead time in order to minimise flood hazard is concerned. Rainfall forecast through numerical weather prediction techniques is the present trend in which researchers across the world are working. Different NWP models are developed and scientists across the world are engaged in calibration and validation of these models with different rainfall observation data. Such studies in the Indian sub-continent has been found to be very limited. Moreover due to the gross inadequacy of surface observation of rainfall in our sub-continent, NWP techniques seem to be a viable alternative for generating useful rainfall input for flood

prediction by coupling them with already developed basin scale hydrological runoff models.

Surface characterization of floodplain in general and river channel in particular has been another area of research related to flood inundation. Researchers all over the world are mostly using the global DEMs freely available in public domain. From reviewed literatures, it has been known that, in the absence of the parent source data, these freely available DEMs are difficult to be edited and most of the time reasons behind abrupt changes in elevation values are not properly understood. Locally generated DEM by stereo photogrammetric techniques have now been used whenever the application demands precision in vertical resolution. It has now become important to compare the capabilities of such locally generated DEMs with respect to the freely available global DEMs especially in the context of floodplain and river channel representations as an input for inundation studies.

Delineation of flood hazard zones or scientific identification of flood prone area is another relatively new domain of research for long term management planning for mitigation of flood hazard. Till date researchers have worked with two approaches of statistical analysis of historical inundation records and by hydraulic flood inundation simulation with respect to different river levels. The limitation with the statistical approach is that it identifies only those areas which have been inundated as per records and does not account for missing records or those areas which in spite of being potentially hazardous have not been flooded till date. On the other hand, the second approach of hydraulic simulation is highly dependent upon accuracy of input model parameters such as resistance parameters, bathymetry etc and may give erroneous results due to data inadequacy and over assumptions. These limitations have given birth to a third rather indirect but logical

approach of flood hazard zonation using remote sensing indices and other field parameters favourable to flooding. Very limited numbers of researchers have been found to have attempted this third approach of multi-criteria flood hazard zonation. Here, although the remote sensing indices are limited in numbers, but there is flexibility in using different field parameters as applicable to the river basin concerned. It has been found that a number of combinations of these parameters have not yet been tried and therefore there is enormous scope of work on this third approach of flood hazard zonation.

Chapter 3
THE STUDY AREA

3.1 INTRODUCTION

The Brahmaputra basin in India, particularly its valley in Assam, represents an acutely flood-prone region characterized by major hazards of flood and erosion that create an annual mayhem of devastations bringing untold miseries to the people and causing colossal loss and damage to public property and infrastructure. Although occurrence of flood has been an age-old phenomenon in the riverine areas of this region, yet the extent of damage caused by the hazard has increased significantly in recent years particularly after the great Assam earthquake of 1950 (Goswami, 1998) which recorded 8.7 on the Richter scale. The Brahmaputra valley had experienced major floods in 1954, 1962, 1966, 1972, 1974, 1978, 1983, 1986, 1988, 1996, 1998 and 2000, 2004 and 2009. With more than 40 percent of its land surface susceptible to flood damage, the total flood-prone area in the Brahmaputra valley is 32 lakh hectares which account for 9.6 percent of the country's total. The floods in Assam are caused by a combination of several natural and anthropogenic factors. The unique environmental setting of the basin vis-à-vis the eastern Himalayas, highly potent

monsoon regime, weak geological formations, active seismicity, accelerated rates of erosion, rapid channel aggradations, massive deforestation, intense landuse pressure and high population growth especially in the floodplain belt, and adhoc type temporary measures of flood control are some of the dominant factors that caused and/or intensify flood damages in Assam (Goswami, 1998). The length of the embankments constructed in this region to provide temporary protection against flood amounts to 28% of that in whole of India (Sarma, 2004). The water yield of the Brahmaputra basin is among the highest in the world (Goswami, 1985). This, together with the limited width of the valley and the abruptly flattened gradient, leads to tremendous drainage congestion and resultant flooding. The scenario is further exacerbated by a plethora of social, economic and environmental factors causing increased vulnerability of people to the flood hazard. The flood problem has three main facets so far as the Brahmaputra is concerned. First, the problem of inundation of riverine areas due to overtopping of banks by the main river and tributaries. Second, the problem of drainage congestion especially near the outfalls of the tributaries during high flood stages of the river. Third, the problem of bank erosion and channel instability. The greatest single casualty due to recurrent floods, accounting for as much as 75 percent of the total flood loss, is the agricultural sector which happens to be the mainstay of the economy. Apart from the Brahmaputra main channel, its tributaries are also enormously contributing to the flood problem. Around 19 major north bank tributaries and 13 major south bank tributaries (Datta & Singh, 2004) form Brahmaputra valley in Assam. Among the north bank tributaries, Pagladia in lower Assam and Jiadhal in upper Assam are regarded as two of most severely flooded tributaries as far as records of last one and half decade goes. However, the single most important cause for frequent occurrence of flood in this region is the

extremely dynamic monsoon rainfall regime in the backdrop of the unique physiographic setting. These two tributary basins have therefore been selected as the study area. Detailed characteristics of these two basins relevant to the present study have been presented in subsequent sections of this chapter.

3.2 THE PAGLADIA RIVER AND ITS WATERSHED

The Pagladia river is one of the major tributaries on the north bank of Brahmaputra river in lower Assam. The Pagladia as the name implies, has been a chronic source of trouble due to annual flood and severe bank erosion leading to frequent changes in its flow path. The flat portion of the main river course originates at the foothills of Bhutan and finally terminates into the Brahmaputra near a village named Lowpara near Hajo in Kamrup district. Its major floodplain lies in two adjacent north bank districts of Nalbari and Baksa.

3.2.1 The basin description

This river system drains an area of 1,674 sq. Km (Brahmaputra Board Master Plan report, 1996) and the drainage area lies between longitudes 91°20' E and 91°42' E and between latitudes 26°14' N and 26°59' N. Out of the total catchment area of 1674 sq. km, area within Indian territory is 1251 sq. km and the rest 423 sq. km lies in Bhutan. The hilly portion of the catchment area is about 465 sq. km of which 423 sq. km are in Bhutan and the rest 42 sq. km lies in Indian territory. The River flows for a length of 19 km in hilly tracts of the Bhutan territory and for the rest 178km, it flows through the Nalbari and Baksa districts of Assam, India. In the hilly portion, slope of the river bed is very steep, being 1 in 75, in the middle reach it is 1 in 200 and in the lower reach, i.e., from Hajo-Nalbari road to outfall it is 1 in 2600. Fig. 3.1 below shows a geo-coded satellite image of the Pagladia Basin.

Based on basin topography, river gradient and joining points of tributaries, the Pagladia river has been divided into three distinct reaches. They are as follows

The hilly reach from *source to Chowki* is almost entirely in Bhutan. It extends nearly 19 kms from the lofty Bhutan hills till it descends on to the plains of Assam. The average gradient of the river in this reach is 1:75.

The middle reach from *Chowki to NH road crossing* is with a milder slope of 1:200 thereby creating bed aggradations and bank erosion. Two tributaries namely Mutanga and Dimla join the left bank of Pagladia in this reach.

The lower reach from *NTR crossing to confluence with Brahmaputra* becomes almost flat with a gradient of 1:2600. This reach being a low lying area is mainly characterized by frequent flooding events during monsoon. Being thickly populated and rich in agriculture production, both the banks of this reach needs attention on management of flood. An important tributary named Choulkhoa joins the Pagladia river.

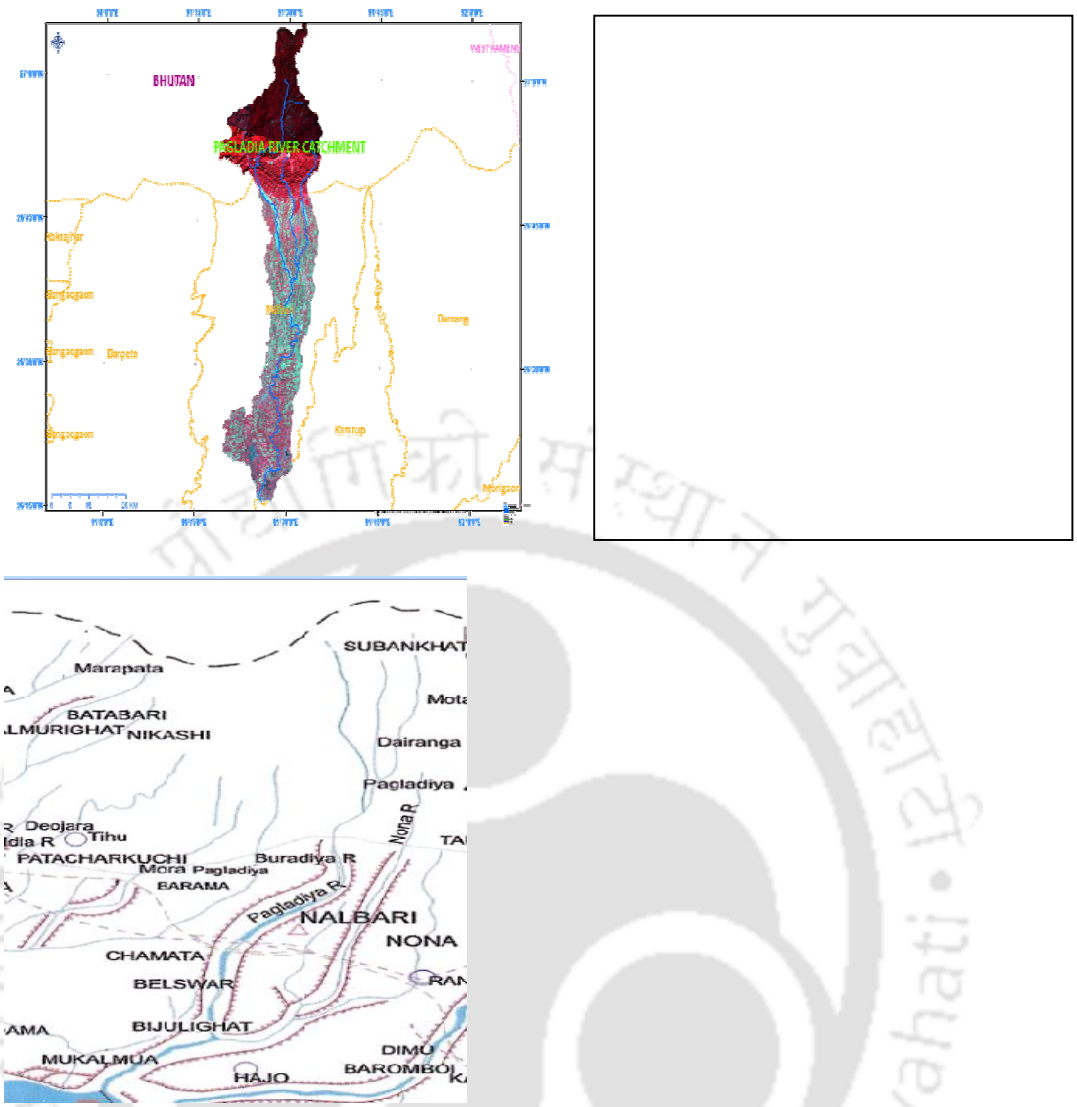

Fig. 3.1: Satellite image (left) and Index map (right) of Pagladia river basin
(The index map source: AWRD, Govt. of Assam)

The table 3.1 below shows the list of major sub-tributaries in the left bank flood plain of Pagladia River. Due to the presence of these sub-tribs, the left bank flood plain of the river has become more prone to frequent flooding due to genesis like more numbers of confluences leading to drainage congestion resulting in flood.

Table 3.1: Important sub-tributaries of Pagladia river

Tributaries (Bank)	**Catchment area in sq. km**	**Length in km**
Mutunga (Left bank)	130	30.00
Dimla (left bank)	48.75	25.50
Nona/Mutanga (left bank)	268	63.00

Chaulkhoa including(left bank) Nona/Mutanga	538	75.00

3.2.2 The Pagladia river system

The Pagladia river sub-system is drained by two major drainage networks namely the Pagladia itself in the western side and the Chaulkhowa system in the eastern side. Following are the major sub-tributaries within the entire river system under study.

The ***Mutunga river*** originates from Bhutan hills and covers a length of about 30 kms. It joins river Pagladia at 28.5 kms below Chowki and about a 1 km upstream of village Thalkuchi where the Pagladia multi-purpose project has been proposed. Mutunga itself is further joined by another tributary named Darranga on its right bank near Barkajuli around 6 kms upstream of the Pagladia – Mutunga confluence. Both these two rivers together covers a drainage area of 130 sq. Kms (Table 3.1).

The Dimla river joins the Pagladia at 13.5 kms down stream of the Mutunga confluence near Kataimari village. The length of the river is 25.5 kms and it drains a relatively narrow valley of 48.75 Sq. Kms (Table 3.1). All these three rivers mentioned above, brings down with them various sizes of sediments to the main channel of Pagladia river contributing to temporal changes to the river morphology of Pagladia river.

The lower reach of the river Pagladia is a thickly populated area and rich in agricultural production but frequently flooded being a low lying area. In this reach an important sub-tributary the Chaulkhowa joins the main river on its left bank in a place called Bijalighat at around 21.5 kms upstream of Pagladia outfall in Brahmaputra. The Chaulkhowa channel is further fed by three important channels namely Ghogra, Nona and Baralia. Among them the Nona river is a meandering with 20 odd loops in both its right and left bank. The Baralia river originates from Nagrijuli tea estate where some

small rivers from Bhutan as underground channels combines together to give rise to the Baralia river channel. The flood plain of Pagladia river starts at a place known as Thalkuchi where the main channel of the river is joined by two more rivers namely Mutanga and Nona. The average elevation of the flood plain at embankment base drops from 71.2 meters to about 44.3 meters at the outfall at Brahmaputra as found out by digital terrain analysis. The main channel traverses a distance of around 64 km for this drop. Thus few major flooding and congestions zones have been identified. Among them the upstream portion of the flood plain i.e the upper middle reach and the lower middle reach of the river the genesis of flood has been found to mainly due to excess run-off and inadequate channel capacity downstream of the confluences. But the lower most part of the flood plain towards the river's outfall with river Brahmaputra. This area comes under frequent flooding zone due to heavy rainfall and subsequent flood discharge in its own upstream catchment.

3.2.3 Meteorology of Pagladia river basin

The Pagladia watershed falls within the climatic zone-I which comprises of North and North east India as well as adjoining parts of Nepal, Bhutan Bangladesh and North Myanmar. The watershed enjoys an average annual rainfall in excess of 2318 mm. Here the rainfall generally occurs in the monsoon months of June to September while the months of November to February are generally dry with occasional winter rains. Sometimes heavy rainfall is experienced in the month of May and October. The climate of this catchment can be described as tropical monsoon climate. As part of the periodical changes of climatic condition in this zone, by the end of May and beginning of June, the south west monsoon enters north eastern region through Bangladesh and establishes itself firmly over the area. The passage of cyclonic storm originating in the bay of Bengal during this period

causes incessant precipitation in the entire Pagladia watershed. It generally occurs in late May or early June and continues up to late September or middle of October. Sometimes land based in situ depressions in Assam, Arunachal Pradesh, Bhutan and adjoining areas also influence heavy precipitation in this watershed. Based on rainfall data available prior to 1994, the watershed experienced an average yearly total pre-monsoon rainfall ranging from 323 mm to 873 mm across different stations and yearly total monsoon rainfall ranging from 632 mm to 2073 mm. A total of 10 rain gauge stations are there in the watershed but most of them are either non functional or having huge data gaps. Hence at present meteorologically, the watershed may be considered as an ungauged one what makes it an appropriate river basin for attempting satellite based NWP models for rainfall prediction as an input to discharge prediction for forecasting of flood.

3.2.4 Hydrology and flood frequency of Pagladia river basin

The watershed has hydro-observation sites in four locations namely Thalkuchi / hahkata, N.T road crossing, Bijalighat and goldighala, out of which presently only the site at NT road crossing is functioning as a gauging site with no discharge measurement. Based on historic data prior to 1990, table 3.2 showing flood frequency results below has been prepared. The Thalkuchi site takes care of the Pagladia upper

Table 3.2: Flood frequency results for Pagladia river

Sl. no	Name of the site	Return Period flood (Cumec)					
		2 Yr	5 Yr	10 Yr	25 Yr	50Yr	100 Yr
1	Thalkuchi	382.33	608.02	757.44	946.23	1086.29	1225.32
2	N.T Road crossing	523.16	713.10	1194.60	1502.23	1708.71	1898.04

reach. The observations in the N.T road crossing site takes into account the combined discharge of Pagladia, Mutunga and Dimla river. This is one of the most important observation sites. The available limited historic data (source: Brahmaputra Board) also reveals the monsoon yield and non-monsoon yield to be 81.44 % and 18.56 % of the annual yield respectively. The gauge-discharge relationship is as follows

$$Q = 3.049\,(G - Go)^{3.976} \quad (3.1)$$

Where,

Q = Discharge in Cumec

G = Observed water level in meter

Go = Water level corresponding to zero discharge

= 49.60 m.

As presently no discharge data available for Pagladia river (Only level data at NTR Crossing site available), hence hydrologically also the basin may be considered as ungauged. This makes it appropriate to study the usefulness of lumped and distributed hydrological models with input of rainfall predicted through NWP models.

3.2.5 The river channel and floodplain morphometry

Morphometry deals with the measurement and mathematical analysis of the configuration of the earth surface in a watershed as opined by Clark, 1966. Drainage or fluvial morphometry, on the other hand denotes the measurements of geometrical properties of the land surface of a fluvial erosion system. The analysis of the hypsography as depicted in figure 3.2 below reveals that around 50 % of the

total basin belongs to the flat (0 m to 500 m elevation) alluvial flood plains. While 20% is in the upper elevation (2250 m to 2500 m) ranges, rest 30% belongs to the mid elevation (500 m to 2000 m) ranges. This steep drop in elevation covering the mid elevation ranges results in bed scour in the interface region between hills and plains producing good amount of silt load further downstream which affects the channel configuration across

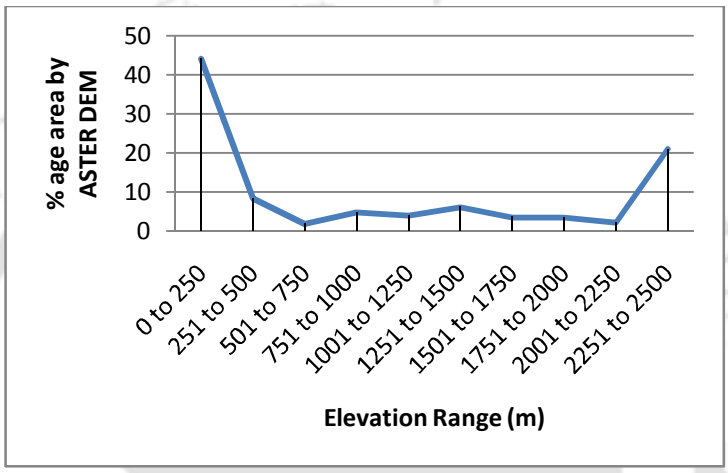

Fig. 3.2: Hypsometric curve of Pagladia basin

Table 3.3: Morphometry of Pagladia river derived from satellite image analysis

Serial no	Morphometric Parameter	Values
1	Form factor	7.26
2	Circularity Ratio	0.26
3	Elongation Ratio	0.42
4	Drainage pattern	Dendritic

the flood plain. Table 3.3 above reveals the other important morphometric parameters of the watershed. The values of both circularity ratio and elongation ratio suggest a fern shaped watershed which also has been found to be the shape when the basin is delineated automatically from CARTODEM by defining only the outlet. The dendrite drainage pattern as revealed is suggestive of little adjustments of underlying structures over a long period of time due to stable igneous kind of rock

formation (Devi, 2000). This indicates that recent geo-morphologic changes taking place in river and floodplain are fluvial in nature.

3.3 THE JIADHAL RIVER AND ITS WATERSHED

The Jiadhal river is another major flood prone north bank tributary of river Brahmaputra in upper Assam. This tributary basin spreads across the states of Assam and Arunachal Pradesh. It is a very flashy river that carries huge amount of silt during flood. The river is more known for the devastation it causes than anything else. The surface and ground water resources of this river basin are very much adequate but very little has been done so far for its development. This river has been a cause of sorrow for the people living in the districts of Dhemaji and Lakhimpur in upper Assam.

3.3.1 The basin description

This river basin spreads across the states of Arunachal Pradesh and Assam and lies between latitude 27°08' N and 27°45' N and longitude 94°15' E and 94°38'E. Total catchment area of the basin is about 1346 sq. Km (Brahmaputra Board Master Plan report, 2000), out of which 306 sq. km lies in the hills of Arunachal Pradesh and the rest 1040 sq. km lies in the plains of Assam. The hill part comprises of nearly 23 % of the overall catchment area of the basin. The basin falls in the West Siang district of Arunachal Pradesh and Dhemaji district of Assam. It is bounded by the Subansiri river basin on its west and north and by the Moridhol river basin on its east. The southern

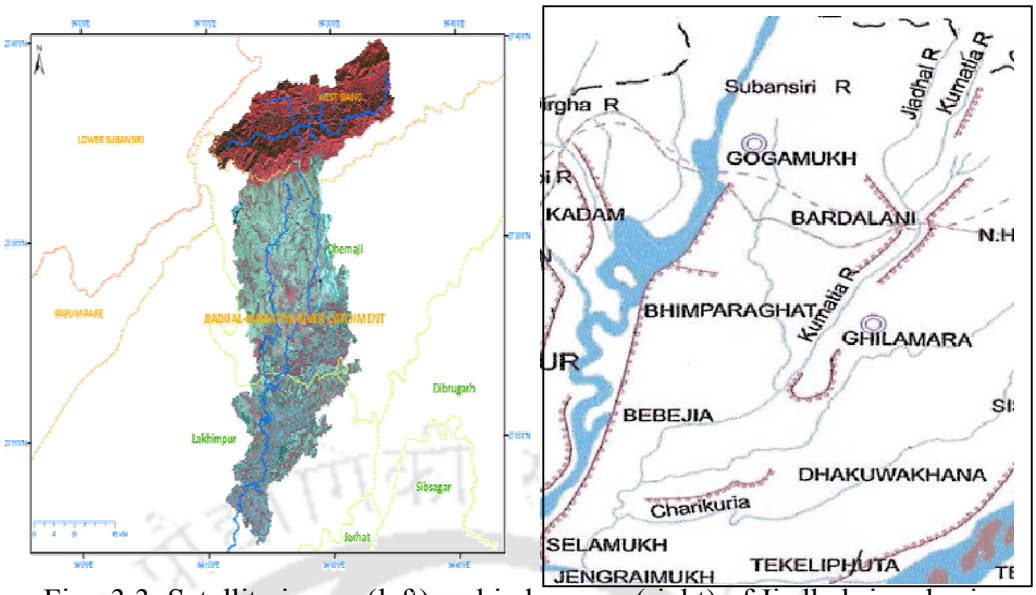

Fig. 3.3: Satellite image (left) and index map (right) of Jiadhal river basin
(Source of index map: AWRD, Govt. of Assam)

side of the river basin is bounded by the Kherkutiasuti, a sub-channel on the northern bank of the Brahmaputra. As far as the geology of the basin is concerned, it is located in the middle Siwalik formation which comprises essentially the sandstone with occasional pebble beds. The lower part of the sub-basin falls in the alluvial formation of the Brahmaputra north bank floodplain. The figures 3.3 above show the river catchment in satellite images.

3.3.2 The Jiadhal river system

The river originates from the lower Himalayan ranges in Arunachal Pradesh at an altitude of about 1247 meters. From its source it flows north – south direction for about 30 kms. The river then takes a west ward turn and take the name Siri, which after flowing for about 27 kms south ward meets two important sub-tributaries namely Sika and Sido in its right bank and further flows for about 8 kms before entering Assam at a place called Jiadhalmukh. In Assam plains the river does not follow a definite course and frequently migrates and changes its course after every flood season. In Assam plains it is joined by three sub-tributaries namely Dihingia, Koran and the most prominent Kumatia. The river finally outfalls into a north bank

sub-channel of river Brahmaputra known as Kherkutia suti at an elevation of 90m from msl. The hilly stretch of river is 65 km long having a average gradient of 1:58 while the plain part is 122 km long with a much flatter gradient of 1: 3389. Table 3.4 below shows five important tributaries of the Jiadhal river system. Considering the topography, gradient and other characteristics the river is divided into two distinct reaches. They are as below:

The **reach from source to Jiadhalmukh** is about 65 km. In this reach the river flows through hilly terrain with steep gradient of about 1:58. The source lies at an altitude of 1247 m and it comes down to about 126 m at Jiadhalmukh. Although many tributaries join the river in this reach, the two sub-tributaries namely Sika and Sido meets the Jiadhal in side Arunachal Pradesh at a place called Tinmukh. In fact downstream of Tinmukh only the river is known as the Jiadhal.

Table 3.4: Important sub-tributaries of Jiadhal river

Tributaries (R/L Bank)	**Catchment area in sq. km**	**Length in km**
Kumatia (Left bank)	74	27.00
Koran (left bank)	223	147.00
Sika (Right bank)	49	14.00
Sido (Right bank)	112	21.00
Dihingia (Right bank)	153	30.00

The **reach from Jiadhalmukh to outfall** flows through the alluvial plains of Assam. The average slope of the river in this reach is about 1:3514. In this reach Jiadhal is joined by three prominent sub-tributaries known as the Dihingia on the right bank and the Kumatia and Koran on the left bank. In this reach the river has

undergone considerable changes due to bank migration, siltation etc. The river causes havoc every year due to flood erosion and bank migration.

3.3.3 Meteorology of the Jiadhal river basin

The Jiadhal sub-basin also falls within the climatic zone 1 which comprises of north and north east part of India, adjoining parts of kingdom of Nepal, Bhutan, Bangladesh and north Myanmar. The annual temperature in this sub-basin varies between 4.2°C and 36.3°C. In this zone the rainfall generally occurs in the monsoon period of June to September where the peak rainfall generally for three main months of June, July and August. Tropical storms and depressions affect the weather in this zone during these monsoon months. This zone experiences pre monsoon shower and thunder storms in the month of April and May. Rainfall observation in Jiadhal sub-basin has been poor due to various factors. There has been few rain gauge stations at places like Ghilamari, Dhemaji, Gerukamukh etc but none of them are maintained by IMD, the principal agency for weather and rainfall observations in India. Moreover majority of the time, these rain gauges remain out of order due to various maintenance issues thereby causing enormous data gaps which is a major hindrance for systematic analysis of rainfall data. That is why Jiadhal basin has been found to be suitable to study the usefulness of rainfall prediction through NWP modelling and its use as an input for hydrological model for prediction of flood under the present research work. With limited historical data availability, it has been found that the pre-monsoon, monsoon, post monsoon and winter rainfall in this river basin are 17.51%, 72.07%, 6.90% and 3.52% of average annual rainfall respectively. As per the recommendation of world Meteorological Organization (WMO), for ideal spatial distribution of rainfall observations, the Jiadhal basin considered as highly inadequately gauged.

3.3.4 Hydrology and flood frequency of Jiadhal river basin

The process of hydrological observation in this river basin started during 1973 when the erstwhile state flood control department installed discharge observation sites at Jiadhalmukh in Arunachal foothills. Another site was installed at railway bridge crossing in the same year of 1973 and was continued till 1976. The site was then shifted down stream to NT Road crossing in the year 1990 and was continued their till 1995. The gauge observation site has been maintained at NT Road bridge in middle reach on Jiadhal- Kumatia main channel till 1995. Due to frequent changes in the river course and other factors leading to severe data inconsistency, logical analysis of gauge and discharge data could not be done after 1995. Hence this basin at present is one of the well known ungauged basins in the north bank of Brahmaputra valley. Frequency analysis with discharge data available till 1995 has been done and presented in the table 3.5 below. Because of extremely limited data of discharge in this river basin, *the*

Table 3.5: Flood frequency results of Jiadhal river

Sl. no	**Name of the site**	**Return Period flood (Cumec)**					
		2 Yr	5 Yr	10 Yr	25 Yr	50Yr	100 Yr
1	N.T Road crossing	598.06	764.78	856.40	955.61	1019.72	1077.00

discharge computed by both the lumped and distributed hydrological models has been validated with the available flood frequency results shown above as part of the present research work. The mean annual yield at Jiadhalmukh is 2718.50 mcm where as the same at NT Road crossing has been computed to be 2407.27 mcm. Again from the analysis with limited data at Jiadhalmukh and NT Road crossing,

dependable annual yield corresponding to 50%, 75% and 90% are 2241 mcm, 1124 mcm and 507 mcm respectively. The gauge-discharge relationship which has been established with limited data (Source: Brahmaputra Board) is

$$Q = 12.784\,(G - Go)^{3.4061} \qquad (3.2)$$

Where,

Q = Discharge in Cumec

G = Observed water level in meter

Go = Water level corresponding to zero discharge

= 123.00 m.

3.3.5 The river channel and flood plain morphometry

In this river basin the analysis of the hypsometry reveals that around 65% of the total watershed belongs to the flat (90 m to 250 m) alluvial flood plains. While 30% is in the upper (751 m to 1247 m) elevation ranges, rest 5% only belongs to the mid (251 m to 750 m) elevation ranges. Because of this enormously low percentage of basin area in the mid elevation ranges, the transition from higher elevation to flat lower elevation is very steep which is the main reason for flashy behaviour of this river system. Table 3.6 below reveals some of the vital morphometric parameters of the river

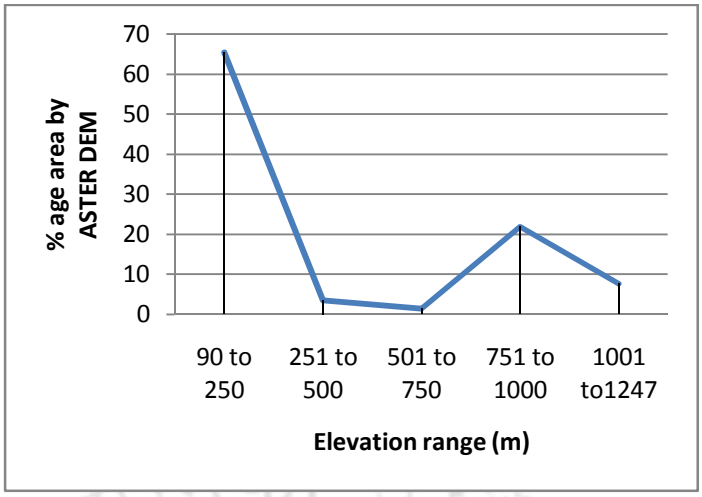

Fig. 3.4: Hypsometric curve of Jiadhal basin

Table 3.6: Values of morphometric parameters of Jiadhal basin

Sl. no	Morphometric Parameter	Values
1	Form factor	5.63
2	Circularity Ratio	0.37
3	Elongation Ratio	0.29
4	Drainage pattern	Dendritic

basin as extracted from satellite image and digital elevation models. Here the values of the circularity ratio and elongation ratio suggest the watershed to be fan shaped. This fact is also supportive towards the flashy nature of the river as in fan shaped rivers high discharge forms faster than that of fern shaped rivers where high discharge formation takes place over a period of time. Good number of confluences in the middle region of Jiadhal- Kumatia also has been found to be responsible for flooding in the middle and lower flood plain of this river lying mainly in the Gogamukh and Dhemaji revenue circles of Dhemaji district of Assam.

Chapter 4
RAINFALL FORECAST BY WRF NUMERICAL WEATHER PREDICTION MODEL

4.1 INTRODUCTION

Accurate prediction of rainfall has been the key for successful forecasting of flood runoff as opined by researchers across the world. Although rain gauges (both manual and automatic) are known to provide the most accurate rainfall measurements (World Meteorological Organization), the usability of measured rain (even if most accurate) is quiet debatable and arguable so far as achieving an actionable lead time of flood forecast is concerned. Although the ground based rainfall measurements have been found to be relatively useful for large regional level river basins with long time of concentration (TOC), their usability has been negated for smaller watersheds with shorter TOC. Apart from ground based direct measurements, some other prime sources rainfall data are ground and space based meteorological RADARs, satellite based rainfall estimates, numerical weather prediction models etc. Both Radar and Satellite based rainfall estimates use some algorithm to derive rainfall from the raw data that the instruments produce. The rainfall estimation techniques are being continously improved and they provide varied accuracy that depends upon the season and geographical location. The rainfall forecast using numerical weather prediction (NWP) models is an emerging area of intense research. The rainfall forecasts from such models are used to increase lead time of flood forecast, particularly for smaller watersheds having shorter flood wave travel time. As discussed in chapter 2 earlier in this research work, researchers across the world are working in different NWP models such as MM5, ARPS, and WRF etc. The weather research forecast (WRF) model, which is a reliable short term forecasting tool (Moustafa *et al.* 2010), has been utilized over the study area in this research work.

4.2 THE WRF MODEL

The Weather Research and Forecasting (WRF) model is a numerical weather prediction (NWP) and atmospheric simulation system designed for both research and operational applications. WRF is supported as a common tool for the university research and operational communities to promote closer ties between them and to address the needs of both. The development of WRF has been a multi-agency effort to build a next-generation meso scale forecast model and data assimilation system to advance the understanding and prediction of mesoscale weather and accelerate the transfer of research advances into operations. The WRF effort has been a collaborative one among the National Centre for Atmospheric Research's (NCAR) Mesoscale and Micro scale Meteorology (MMM) Division, the National Oceanic and Atmospheric Administration's (NOAA) National Centers for Environmental Prediction (NCEP) and Earth System Research Laboratory (ESRL), the Department of Defense's Air Force Weather Agency (AFWA) and Naval Research Laboratory (NRL), the Centre for Analysis and Prediction of Storms (CAPS) at the University of Oklahoma, and the Federal Aviation Administration (FAA), with the participation of university scientists.

The Advanced Research WRF (ARW) modelling system has been in development for the past few years. The current release is Version 3, available since April 2008. The ARW is designed to be a flexible, state-of-the-art atmospheric simulation system that is portable and efficient on available parallel computing platforms. The advanced research WRF has been found to be suitable for wide range of applications such as Real time NWP, rainfall forecast research, data assimilation research, regional climate research etc. The weather forecast using NWP models is an emerging area and lot of R & D happening in this area. The rainfall forecasts

from such models are used to increase lead time of flood forecast, particularly for smaller tributary watersheds.

4.2.1 The model description

The WRF modelling system consists of four major programmes namely the WRF pre-processing system (WPS), WRF variational data assimilation (WRF Var DA) system, advanced research WRF (ARW) solver and the Post-processing and

The dynamic solver uses a time-split integration scheme. Generally speaking, slow or low-frequency (meteorologically significant) modes are integrated using a third-order Runge-Kutta (RK3) time integration scheme, while the high-frequency acoustic modes are integrated over smaller time steps to maintain numerical stability. The horizontally propagating acoustic modes (including the external mode present in the mass-coordinate equations using a constant-pressure upper boundary condition) and gravity waves are integrated using a forward-backward time integration scheme, and vertically propagating acoustic modes and buoyancy oscillations are integrated using a vertically implicit scheme (using the acoustic time step). Klemp *et al.* 2007 demonstrated that these integration techniques appear robust over a wide range of scales, from sub cloud to synoptic. Here the time splitting were similar to what was first developed by Klemp and Wilhelmson in 1978 for leapfrog time integration. This time split approach was extended to the third order Runge Kutta (RK3) scheme as described by Wicker and Skamarock in 2002. The primary differences between the earlier implementations described in the references and the ARW implementation are associated with our use of the mass vertical coordinate and a flux-form set of equations, as described in Klemp *et al.* 2007, along with our use of perturbation

variables for the acoustic component of the time-split integration. The acoustic-mode integration is cast in the form of a correction to the RK3 integration.

The dynamic solver uses a time-split integration scheme. Generally speaking, slow or low-frequency (meteorologically significant) modes are integrated using a third-order Runge-Kutta (RK3) time integration scheme, while the high-frequency acoustic modes are integrated over smaller time steps to maintain numerical stability. The horizontally propagating acoustic modes (including the external mode present in the mass-coordinate equations using a constant-pressure upper boundary condition) and gravity waves are integrated using a forward-backward time integration scheme, and vertically propagating acoustic modes and buoyancy oscillations are integrated using a vertically implicit scheme (using the acoustic time step). Klemp *et al.* 2007 demonstrated that these integration techniques appear robust over a wide range of scales, from sub cloud to synoptic. Here the time splitting were similar to what was first developed by Klemp and Wilhelmson in 1978 for leapfrog time integration. This time split approach was extended to the third order Runge Kutta (RK3) scheme as described by Wicker and Skamarock in 2002. The primary differences between the earlier implementations described in the references and the ARW implementation are associated with our use of the mass vertical coordinate and a flux-form set of equations, as described in Klemp *et al.* 2007, along with our use of perturbation variables for the acoustic component of the time-split integration. The acoustic-mode integration is cast in the form of a correction to the RK3 integration.

in 2012 from that in 2011. Thus like the previous river basin in lower Assam region, here in this upper Assam river basin also, WRF rainfall prediction has performed satisfactorily especially after assimilation of land surface and weather parameters from local sources. The results presented in this chapter primarily suggests that usability of WRF derived rainfall and the TRMM measured rainfall remains similar till local data gets assimilated into the WRF model. The WRF derived rainfall prediction significantly improves once the weather parameter at local level gets assimilated. The next chapter discusses the usability of this WRF derived rainfall prediction as the prime input for discharge prediction leading to prediction of flood in river basin level.

Chapter 5
FLOOD DISCHARGE COMPUTATION BY LUMPED AND DISTRIBUTED HYDROLOGICAL MODELS USING WRF DERIVED RAINFALL INPUTS

5.1. THE LUMPED RATIONAL MODEL

Among the most well known lumped runoff models, we have used the Rational model developed by Emil Kuichling in 1889. Although this model was developed long back and has certain computational limitations, yet it is widely used due to its simplicity (Zoppou 2001; Hayes and Young, 2006). Moreover as the research focus in the present study is more concentrated towards accurate rainfall prediction through numerical weather prediction model as a vital input for approximate computation of river discharge leading to flood forecasting, hence it was though that the lumped rational model with its sources of errors would still be useful

especially when it is used in combination with a relatively accurate and precise distributed hydrological model like the HEC-HMS.

5.1.1 Model description and parameters

The presently used form of the rational model is given as

$$Q = 0.0028\ C\ I\ A \quad (5.1)$$

Where

Q = Peak discharge (cumec or m^3 / s)

C = Discharge coefficient (A fraction implying the percentage of total rainfall getting converted to run-off)

I = Rainfall intensity (mm / hr) for a duration equal to the time of concentration (TOC).

A = Area of the watershed or basin (Ha)

Another important factor associated with this rational model is the time of concentration (TOC) of the watershed or basin which is the time for water to travel from the most remote point of the watershed to its outlet. Time of concentration as per Kirpich equation is given by

$$T_c = 0.0195\ L^{0.77} S^{-0.385} \quad (5.2)$$

Where

T_c = Time of concentration (min)

L = Maximum length of flow (meters)

S = The watershed slope (% age)

The discharge coefficient C is generally decided based on land cover characteristics, slope and the hydrologic soil group as per USDA classification system. Table 5.1

below depicts some portion of this classification which has been used in the present study for computation of C in for the rational method for peak discharge calculation.

Table 5.1: USDA classification for discharge coefficient

Hydrologic soil groups	**A**			**B**			**C**			**D**		
Slope Range (%)	**0 – 2**	**2 - 6**	**> 6**	**0 – 2**	**2 - 6**	**> 6**	**0 – 2**	**2 - 6**	**> 6**	**0 – 2**	**2 - 6**	**> 6**
Land cover												
Forest	0.05	0.08	0.11	0.08	0.11	0.14	0.10	0.13	0.16	0.12	0.16	0.29
Agriculture	0.08	0.13	0.16	0.11	0.15	0.21	0.14	0.19	0.26	0.18	0.23	0.31
Rural Settlement	0.25	0.28	0.31	0.27	0.30	0.35	0.30	0.33	0.38	0.33	0.36	0.42
Urban settlement	0.33	0.37	0.40	0.35	0.39	0.44	0.38	0.42	0.49	0.41	0.45	0.54

Thus discharge co-efficients C for both the river basins have been calculated based on the values given in the table 5.1 above and basin area A is obtained from watershed boundary delineated in GIS platform from satellite data and other contour and drainage maps. The basins were also further subdivided for different prominent river reaches with separately calculated TOC as depicted in figure 5.1 below. Rainfall intensity I for the duration equal to the time of concentration has been computed by averaging the

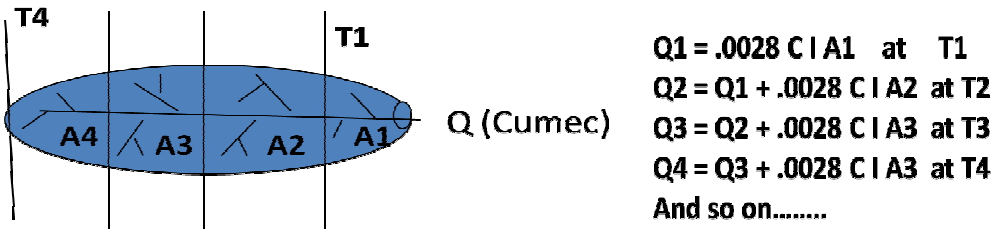

Fig 5.1: Basin partitioning based on prominent river reaches for rational model

9km * 9km WRF derived gridded 3 hourly values into hourly rate of rain spread across the basins. Thus the cumulative daily peak discharge Q have been computed for all the selected low, moderate and high rainfall dates of three peak monsoon months of 2011 and 2012.

5.2. THE DISTRIBUTED HEC-HMS MODEL

This model has been developed by the Hydrologic Engineering Centre of the US army corps of engineers for studying natural hydrologic response of a system of streams or a watershed to a certain rainfall event. A physically based distributed hydrologic model forms the core of HEC-HMS. The model is designed to simulate the precipitation run-off processes of dendritic drainage systems of watersheds (USACE, 2005). The physical representation of the watershed is accomplished with a basin model. Different hydrologic elements are connected in a dendritic network to simulate run-off processes. A variety of methods are embedded for simulating infiltration losses, transforming excess precipitation into surface runoff, calculating base flow contribution to sub basin outflow and flow routing.

5.2.1 Model description and parameters

Two main components that are being used in the present study are the rainfall to run-off conversion component and the flow routing component. The first component is based on Soil Conservation services (SCS) curve number (CN) method which gives us the surface run-off at certain upstream locations where as the second component is based on Muskingum flow routing equations that gives us the corresponding flow at different downstream locations. The execution of both

the above mentioned components has been done in GIS platform. A number of flood related studies have shown that this model performs well (Anderson *et al.* 2002*;* Knebl *et al.* 2005).

The SCS- Curve number (CN) equation is given by

$$Q = \frac{(P - I_a)^2}{P - I_a + S} \tag{5.3}$$

Where

Q =Runoff (m)

P =Rainfall (m)

S = Potential maximum soil moisture retention after beginning of runoff (m)

Ia = Initial abstraction (m) i.e the amount of water before runoff such as infiltration, rainfall interception by vegetation etc. Generally *Ia* is taken as 0.2 *S*

In the curve number method the S and the curve number CN is related as

$$S = \frac{1000}{CN} - 10 \tag{5.4}$$

The value of CN ranges from 30 to 100. Lower numbers indicates low runoff potential and higher numbers indicate increase in runoff potential. Low CN values also indicate good soil permeability.

The flow routing component is taken care of by the above mentioned Muskingum hydrologic routing. As the term “hydrologic” suggests, this method ignores the

momentum equation and based solely on the continuity equation. The peak is attenuated as a result of diffusion caused by storage effect, which is given by

$$Q = XI + (1 - X)O \tag{5.5}$$

$$S = KQ \tag{5.6}$$

Where

K is the travel time between two channel sections and X is a dimensionless factor between 0.0 to 0.5 that weighs the influence of the inflow and outflow hydrographs on the storage within reach.

Substituting the storage equation into continuity equation yields

$$O_2 = C_0 I_2 + C_1 I_1 + C_2 O_1 \tag{5.7}$$

Where

$$C_0 = \frac{KX - 0.5\nabla t}{K - KX + 0.5\nabla t} \tag{5.8}$$

$$C_1 = \frac{KX + 0.5\nabla t}{K - KX + 0.5\nabla t} \tag{5.9}$$

$$C_2 = \frac{K - KX - 0.5\nabla t}{K - KX + 0.5\nabla t} \tag{5.10}$$

The sum of these three coefficients is unity.

The critical part of the calculation is to estimate suitable values of K and x. These values should be obtained by calibrating to available sets of measured inflow and outflow hydrograph data for the channel reach. In case of non availability of data, the value of x between 0.2 and 0.5 is recommended (Hydrologic Engineering Centre, 1990).

Once K and x are known for a channel reach, the computational procedure to obtain the outflow hydrograph is as follows

Step 1: Discretization of the inflow hydrograph in time increment of ∇t .

Step 2: Calculation of the three coefficients.

Step 3: Computation of the outflow hydrograph with Muskingum equation at the end of the channel reach.

Step 4: Repeating of step 3 till the end of the inflow hydrograph is reached.

5.2.2 Geospatial approach followed in building the distributed model

In the present study the methodology that has been followed comprises of following main components.

(a) Creation of geo-spatial layers as required for both the lumped rational model and the distributed HEC-HMS model. These are Basin boundary, Drainage; Land cover, Soil, topography etc. Satellite data of different spatio temporal resolutions such as LISS-III, LISS-IV and CARTOSAT-I have been used. Critical parameters such as basin area, time of concentration, coefficient of discharge etc have been calculated.

(b) Running of rational model by integrating daily average rainfall intensity from grid based WRF rainfall forecast. Here it has been assumed that intensity of

rainfall is evenly distributed across the study area. Peak daily discharges were obtained.

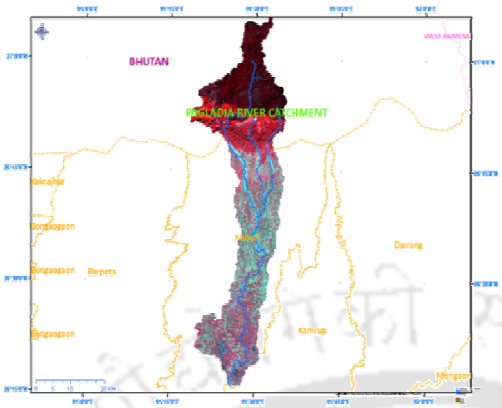

Fig 5.2 (a): Pagladia Basin image

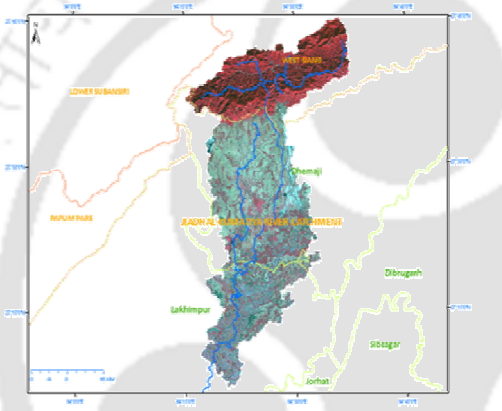

Fig 5.2 (b): Jiadhal Basin image

(c) Creation of the HEC-HMS basin model and its integration with the spatial rainfall forecast generated by WRF rainfall forecasting model to finally run the model in order to generate outflow hydrographs in different time steps of 10 min, 15 min etc.

The important steps that were followed during building the distributed HEC-HMS model set up are Curve number grid generation by integrating land cover and soil for assignment of soil groups, Stream and DEM processing, Generation of CN grid raster, basin lag time calculation, routing parameters K and x assignment etc.

Figure 5.2 and figure 5.3 below explains the work flow of the quasi distributed model and its output.

5.3. VALIDATION OF FLOOD DISCHARGE COMPUTED BY BOTH LUMPED AND DISTRIBUTED HYDROLOGICAL MODELS

Once both the lumped and distributed models were built for the basins of Pagladia and Jiadhal rivers, the geospatially gridded rainfall values as derived from the WRF numerical prediction model (Chapter 4) were used as the prime dynamic input for both the modelling approaches. Both the lumped and the distributed models were run for all the selected dates of low, medium and high rainfall (as presented in Chapter 4) of June, July and August for both years of 2011 and 2012. The lumped rational model

5.3.2 Discharge validation in Jiadhal river basin in upper Assam

Just like the Pagladia basin as discussed in the previous section, here also discharges have been computed for a total of 18 selected rainfall events spread across three peak monsoon months of June, July and August for two consecutive monsoon seasons of 2011 and 2012. The WRF derived spatially distributed rainfall prediction values were used for running both the lumped rational model and the distributed HEC-HMS model. Just like the Pagladia river, here also the spatially distributed rainfall values were totalled and averaged to be used in the lumped model where as they were used as individual gridded values to be used in the distributed model. Same format for presentation of the results of model performance have been followed as done in the previous section. Figure 5.11 and 5.12 below present the results for the month of June in Jiadhal river for both the monsoon seasons of 2011 and 2012. Here it has been found that the discharge

computed by the lumped approach has not tallied satisfactorily with the observed river stage during June, 2011 where as performance of the distributed approach has been satisfactory during the same month. On the other hand during June, 2012, although the performance of the discharge computed by the lumped rational method got relatively improved, but still the performance of the distributed approach was found to superior to that of the lumped approach during the month of June, 2012.

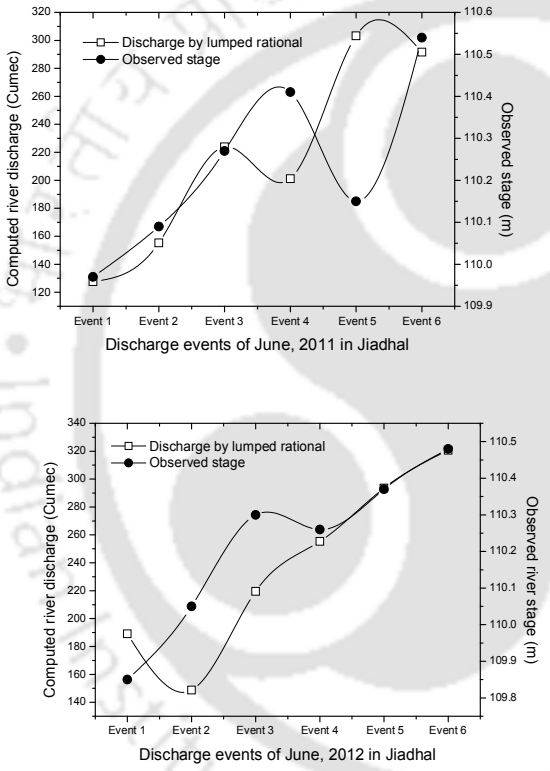

As part of the primary validation in the month of July, the discharge computed by the lumped rational method has been found to perform moderately against observed river stage during 2011 but has performed satisfactorily during 2012 as depicted in figure 5.13 (a). So far as discharge computed by the distributed approach is concerned, some contradictions have been observed during July, 2011 but likewise the case of the lumped rational method, the distributed HEC-HMS model has also performed very satisfactorily during July, 2012 as shown in figure

5.13 (b). Again as part of the secondary validation, the common trend of overestimation by the lumped model continued in the month of July also, although the flood discharge computed by the distributed HEC-HMS model were also found to be closer in majority of the occasions as depicted in figure 5.14 (a). A gradual upward trend is seen from both the lumped and the distributed approach from the low rainfall dates towards the high rainfall dates. The correlation has also been found to be satisfactory in both the seasons as shown in figure 5.14 (b), although the discharges by lumped and distributed model were in relatively better agreement in 2012 than that in 2011. The discharges computed were well spread across the spectrum between less than 2 year return period and little above 10 year return period. Figure 5.15 and 5.16 below presents the corresponding results for the month of August in Jiadhal river basin. Here as part of primary validation with observed river stages, the discharge computed by the lumped approach has performed relatively better during August, 2012 than during August, 2011 as depicted below. The

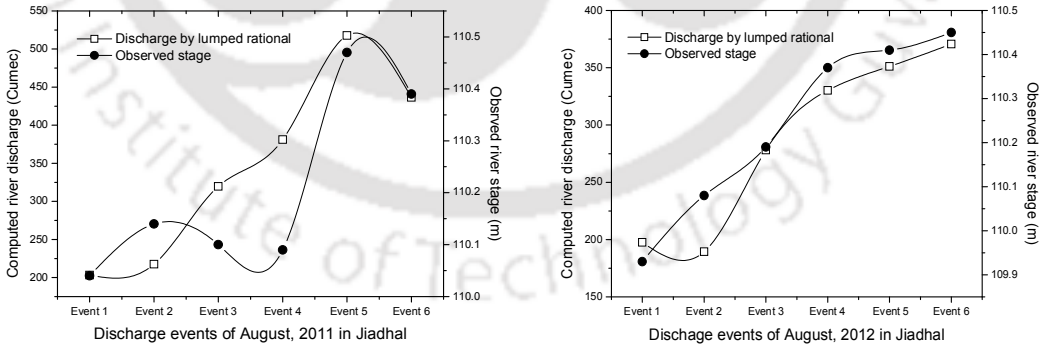

Figure 5.15 (a): Validation of daily peak discharge computed by lumped rational method against observed river stage during August, 2011 (left) and August, 2012 (right) in Jiadhal river

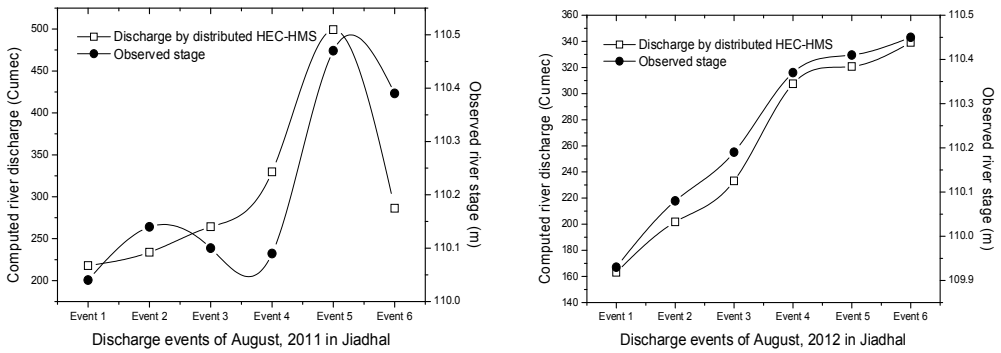

Figure 5.15 (b): Validation of daily peak discharge computed by distributed HEC-HMS model against observed river stage during August, 2011 (left) and August, 2012 (right) in Jiadhal river

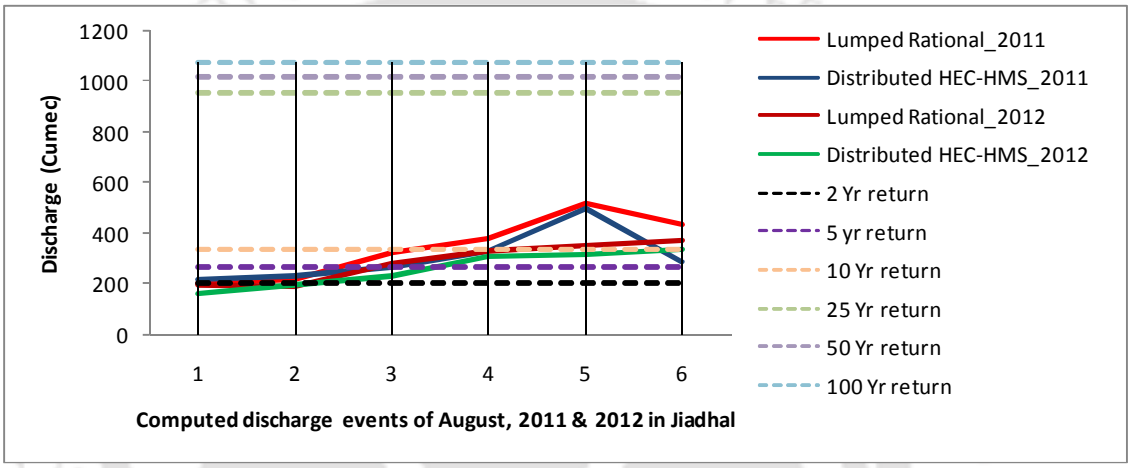

Fig 5.16 (a): Discharge validation for month of August in Jiadhal river

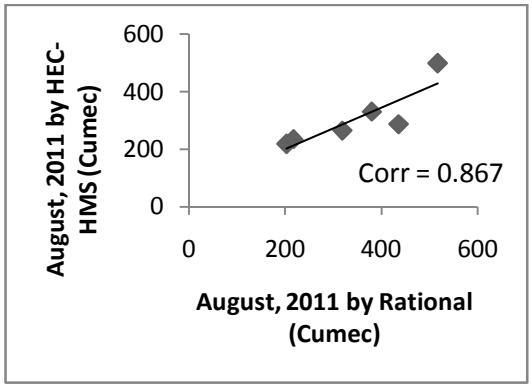

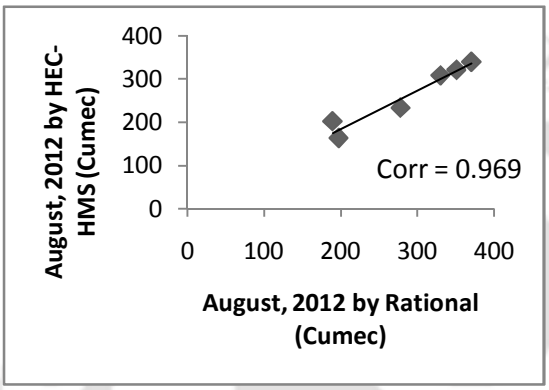

Fig 5.16 (b): Rational Vs HEC-HMS in 2011 (left) and 2012 (right) for August in Jiadhal river

distributed HEC-HMS model on the other hand has performed satisfactorily against the observed river stage both during August, 2011 and August, 2012 which is apparent from figure 5.15 (b) above. As part of the secondary evaluation, finally in the month of August also the lumped rational method has been found to overestimate the HEC-HMS model in majority of the occasions especially that of high and medium rainfall days. As depicted in figure 5.16 (a), it has been found to be common in both the consecutive monsoon season of 2011 and 2012 in this river basin. Likewise the previous two monsoon months, in August also the computed discharges were found to be ranging between the available flood frequency of 2 year return period and 10 year return period although it has overshoot the 10 year return period in some occasions where available ground reports are also known to be suggestive of major flood in Jiadhal basin during August, 2011. There was no major flood event during August, 2012 and computed values also suggest the same.

With this the discharges computed by both the lumped and the distributed models have been validated for both the river basins under consideration for two consecutive monsoon season of 2011 and 2012. Following major observations have been made.

- Even in the absence of observed discharge, the computed discharges have been validated meaningfully with the available stage data of the concerned dates.
- Between the two approaches of discharge computation, the distributed approach computed discharges have tallied satisfactorily with the observed stage data in majority of occasions whereas the lumped rational method derived discharges have tallied in a mixed manner.
- Although the same WRF rainfall prediction has been used as the input in both the models, the lumped model derived discharge has in majority of occasions overestimated the peak of the hydrograph generated by the distributed model.
- All in all the discharge computed by both the approaches have been found to ranging between the available flood frequency of 2 year return period and 10 year return period in both the river basins.
- In majority of occasions, the monthly correlation between the peak flow computed by the rational method and the HEC-HMS model have been found to have improved in 2012 from that in 2011.
- A number of major flood events in these two years, as per ground reports, has also been reflected encouragingly by the discharge values computed by both the models with input from WRF precipitation datasets.

As the non-availability of observed discharge data was a major handicap for calibration and validation of run-off models, the indirect method of estimating

discharge using rating curves had to be implemented which brought to forms the importance of updating river cross section data. As regular hydrographical survey for river cross section is a tedious and cost intensive process and is seldom available for researchers, the next chapter is dedicated towards extraction of river cross sections from digital elevation model data from different sources and at different horizontal and vertical resolution.

Chapter 6
EXTRACTION OF RIVER CHANNEL AND FLOOD PLAIN TOPOGRAPHY BY DIGITAL ELEVATION MODELS

6.1 INTRODUCTION

Various parts of Brahmaputra valley in Assam get flooding almost every year due to high flows both in Brahmaputra main channel as well as the tributaries on north as well as south bank causing small, medium and large scale inundation in the adjoining flood plains. The flooding in the flood plains of Assam is also characterized by frequent changes in river course, rapid bank line erosion, breaching of embankments etc. As the flood plains of Assam are dominantly a flat alluvial terrain, a small increase in water surface elevation can make a big change in the extent and spread of flood inundation. Hence a common but very difficult question often needs to be answered is what will be the inundation spread for a particular magnitude of flood in terms of discharge and gauge or level. Precise extraction of the floodplain topography in general and river profile (both longitudinal and transverse) are proven to be important morphological information by many previous authors including Moore *et al.* 1991 for flood inundation studies related to identification of flood hazard zones. The horizontal and vertical

resolution of satellite based digital elevation model (DEM) plays important role in near realistic characterization of flood plains from inundation point of view. Hence the appropriate selection of the digital elevation model data is of utmost importance for flood plain studies. The earth observations systems of some advanced nations have carried out satellite missions for mapping the earth topography and are generous enough to release the respective DEMs of different spatial resolutions (with some encryption from developer side) in public domain for benefit of researchers across the world. Shuttle Radar Topography Mission (SRTM) and Advanced Space borne Thermal Emission and Reflection (ASTER) are two such global satellite missions, the DEMs of which researchers across the world are extensively using for different research and applications due to their easy and cost-free availability in public domain. The SRTM is a RADAR derived DEM available in 90 m spatial resolution where as ASTER is thermal emission based DEM available in 30 m resolution. With an average vertical error of 16 m (Sanders *et al.* 2007), the SRTM DEM has not been found to be suitable for accurate extraction of minor undulations in flat alluvial flood plains. On the other hand ASTER has been claimed to be relatively useful for extraction of river geometry (Gichamo *et al*. 2011) on a stable river in Hungary. But no conclusive literature exists to prove its suitability for unstable alluvial floodplains as that exists in basins of Brahmaputra valley. Apart from these freely available global DEMs, researchers are also using local DEMs generated through photogrammetric techniques using pairs of satellite stereo images. Usability of such DEMs for hydrological applications have been reported by researchers like Theiken *et al*. 1999 and Fraser *et al*. 2002. Pair of stereo images from an Indian satellite CARTOSAT-I launched in 2005 has been used for generation of DEM for variety of applications including

hydro-geomorphologic studies. Krishnamurthy *et al*. 2008 have worked on its planimetric and vertical accuracy and have reported an average vertical accuracy between 3.8 m to 7.3 m in different topographic condition. In the present research work we have tried a comparison of terrain extraction capabilities between the ASTER global DEM and photogrammetrically generated CARTOSAT-I stereo DEM in two flood prone alluvial river basins of Brahmaputra valley with special focus on extraction of river cross sections and longitudinal profile. Following sections of this chapter are devoted to important technical details, processing steps etc related both the digital elevation models and extraction of terrain attributes such as river profiles, basin hypsography etc for both the river basins under consideration followed by results of their comparison and discussion on their relative suitability for generation of these terrain attributes as input for flood hazard management.

6.2 THE ASTER DEM

The Advanced Space borne Thermal Emission and Reflection Radiometer (ASTER) which is onboard the National Aeronautics and Space Administration (NASA)'s Terra satellite is one of the popular sources of global DEM. This ASTER sensor has been acquiring topographic data since the year 2000 (Hirano *et al*. 2003).

6.2.1 Data acquisition by ASTER

The ASTER system is equipped with 14 nadir looking spectral bands starting from visible, near infra-red (NIR), short wave infra-red (SWIR) to thermal infra-red (TIR) in addition to a backward looking VNIR (visible & near infra-red) band. The bands which are used to acquire the topographic data are the VNIR bands having a spatial resolution of 15 m. The nadir viewing band is called 3N and the backward

looking band is called 3B as shown in figure 6.1 below. Two successive images of the same area are acquired with a time interval of approximately 55 seconds by each sensor

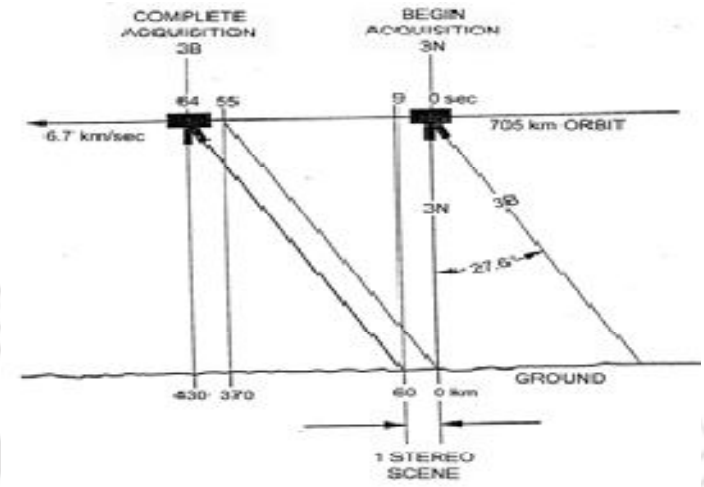

Fig.6.1: Imaging orientation and data acquisition timing by ASTER

6.3 THE CARTOSAT-I STEREO DEM

CARTOSAT-I is the eleventh satellite in the Indian Space Research Organisation's (ISRO) Indian Remote Sensing (IRS) series, and it is the first with high-resolution stereo imaging capabilities. As a dedicated stereo collection platform, CARTOSAT-I is meant to support the extraction of 3D features and Digital Elevation Models. CARTOSAT-I data is offered in a convenient 'Ortho kit' format (NRSA, 2005), which is a radiometrically corrected TIFF product with Rational Polynomial Coefficients (RPCs) for the two images. Due to the simplicity of data handling for RPC-based products, some of the major photogrammetric software vendors have already incorporated support for CARTOSAT-I ortho kit data into their products. While the provision of data in TIFF+RPC format promises a very shallow learning for working with CARTOSAT-I stereo imagery, experience with previous IRS platforms has shown that some ground control is required to achieve acceptable positional accuracy (Lutes, 2006). In the present

study also ground control points (GCP) have been incorporated (through GPS survey) in the DEM processing in order to achieve positional accuracy.

6.3.1 CARTOSAT-I platform, sensor and orbit characteristics

CARTOSAT-I is a dedicated stereo platform. While it can be configured to collect imagery in a monoscopic mode, the sensor payload consists of a pair of 2.5 meter panchromatic camera assemblies mounted in a stereo viewing configuration much like the ASTER sensor onboard TERRA (Abrams *et al.* 2002) satellite. The two camera assemblies onboard CARTOSAT-1 is known as the 'Fore' camera and the 'Aft' camera. The 'Fore' camera points 26 degrees ahead of nadir, while the Aft camera points back 5 degrees behind nadir. This gives excellent stereo viewing geometry, with an average base-to-height ratio of approximately 0.62 at the satellite altitude. Table 6.1 below describes some key characteristics of the CARTOSAT-I sensor. CARTOSAT-I

Table 6.1: CARTOSAT-I sensor specifications

Sensor Specifications	**Camera**	
	Fore (+ 26°)	**Aft (- 5°)**
Spatial Resolution	2.5 m cross track 2.8 m along track	2.2 m cross track 2.2 m along track
Spectral Sensitivity	500 – 850 nm	500 – 850 nm
Swath width	29 km	26 km
Number of detector element	12000	12000
Detector size	7*7 µm	7*7 µm
Focal length	1945 mm	1945 mm
Camera Field of View (FOV)	2.4°	2.4°
Detector integration time	0.336 ms	0.336 ms

operates, like many other remote sensing platforms, in a near-polar, circular sun synchronous orbit at an average altitude of 618 km. Some key orbit characteristics are presented in Table 6.2. The orbit revisit time is 126 days, but a 5-day revisit time can be achieved by tilting the satellite to the east or west of nadir. Given the orbit characteristics and sensor geometry, it can be seen that at the equator, approximately 53 seconds will elapse between collection of the forward and aft scenes. Due to Earth rotation, however, the satellite ground track will have moved by 26 kilometres to the west in that time. To keep the aft camera following the same ground track as the fore camera, it is necessary to employ yaw steering onboard the satellite. This capability is also used to allow monoscopic collection; in this mode, yaw steering is used to keep the

Table 6.2: CARTOSAT-I orbit characteristics

Nominal altitude	618 km
Orbit per day	14
Orbit repetition	126 days
Revisit time	5 days
Equatorial crossing on descending pass	10:30 am local time
Orbital eccentricity	0.001
Orbital inclination	97.87°

aft camera following a path contiguous with the fore camera, thus covering a 55 km wide monoscopic swath. Monoscopic products are not used in the present study, but CARTOSAT-I with 2.5 m stereo can be tasked to collect them if requested.

6.3.2 CARTOSAT-I stereo data processing for DEM generation

In the present study, CARTOSAT-I stereo pair images acquired during November, 2011 of both Pagladia and Jiadhal river basins were considered with rational polynomial coefficients (RPCs) inputs procured from NRSC Data Centre (NDC). Leica Photogrammetric Suite (LPS version 9.0) is used for triangulation, DTM extraction and ortho-rectification processes. Analysis of 2-D geometry and radiometry is carried out using ERDAS Imagine software. The DEM has been extracted from both the stereo-pairs using the LPS module. The posting interval for the regular DEM is 10 m and generated for the full overlap. Ground control points (GCPs) and tie points were also incorporated. A total of 11 nos GPS points were collected for both the basins each using a single frequency geodetic GPS receiver in relative positioning mode. While generating the stereo model, eight out of eleven ground points were used as Ground control points (GCPs) where as three remaining points were used as tie points as shown in figure 6.3 below. The exterior orientation parameters were refined while using the 8 nos GCPs through triangulation. And after triangulation, the CARTOSAT-I stereo DEMs for both the river basins were generated. Figure 6.4 below shows the CARTOSAT-I stereo DEM generated for both the Pagladia and the Jiadhal river basin classified as per their prominent elevation ranges. For evaluation of both the DEMs

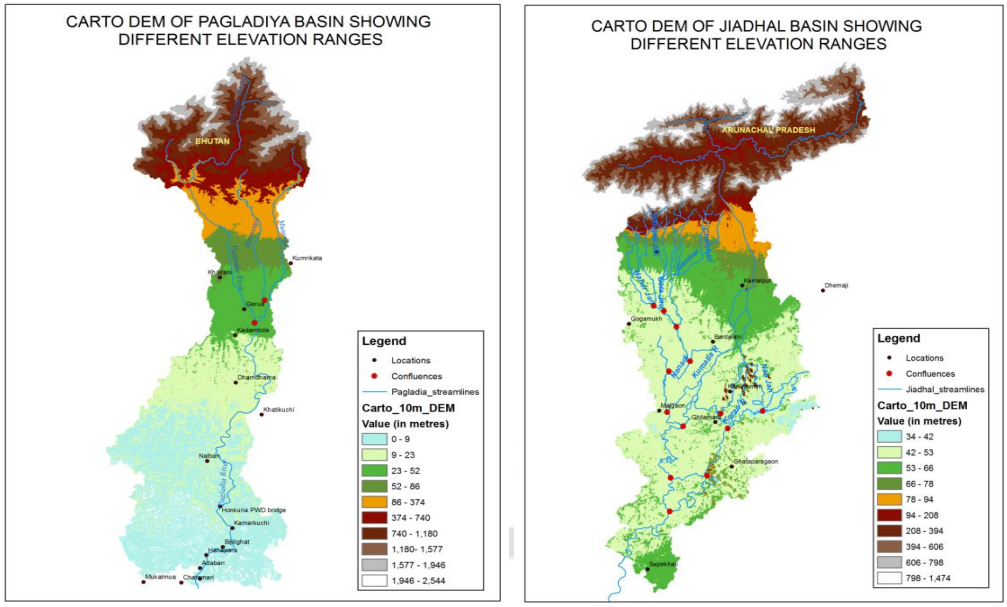

Fig.6.4: CARTOSAT-I stereo DEM of Pagladia (left) and Jiadhal (Right) river basins

generated using CARTOSAT-I stereo data, all the ground points used as both GCPs as well as tie points were studied. The comparison of ground height generated by the DEM and the ground height collected by the geodetic single frequency GPS has been presented in Table 6.4 below. This comparison shows in all the occasions the elevation values derived from the CARTOSAT – I DEM generated without incorporating the GCPs and tie points, have grossly overestimated the GPS recorded ground heights. On the other hand, the elevation derived from the DEM generated by incorporating the GPS collected GCPs have been found to be satisfactorily closer to the values of elevation recorded by the single frequency GPS receiver. A similar comparison done for the DEM of Jiadhal river basin has also shown similar results. Figure 6.5 below shows entire work flow for generation of CARTOSAT-I stereo DEM.

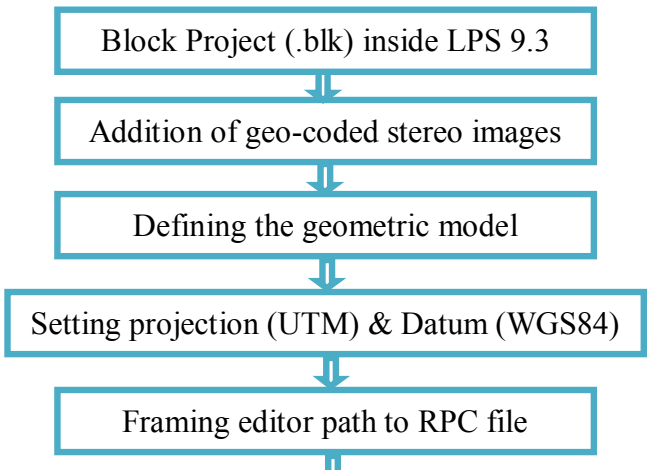

Fig. 6.5: CARTOSAT – I stereo DEM generation workflow

6.4.1 Longitudinal river bed profile extraction

Here the river and the reach network layer is represented by the stream centre line layer. The stream centre line layer is used for assigning river stations to cross sections and to display as a schematic in the HEC-RAS geometric editor. Similarly the location, position and extent of cross sections are represented by the cross sectional cutline layer. These cut lines are always placed perpendicular to the direction of flow. While these cut lines are the planner locations of the cross-sections, the station elevation data are extracted along the cutline from the DTM generated out of both the ASTER and the CARTOSAT – I stereo DEM. Figure 6.6 below shows the comparison between the longitudinal profiles of Pagladia river as extracted from both ASTER global DEM and CARTOSAT-I stereo DEM. Here it has been found that in the 85 km

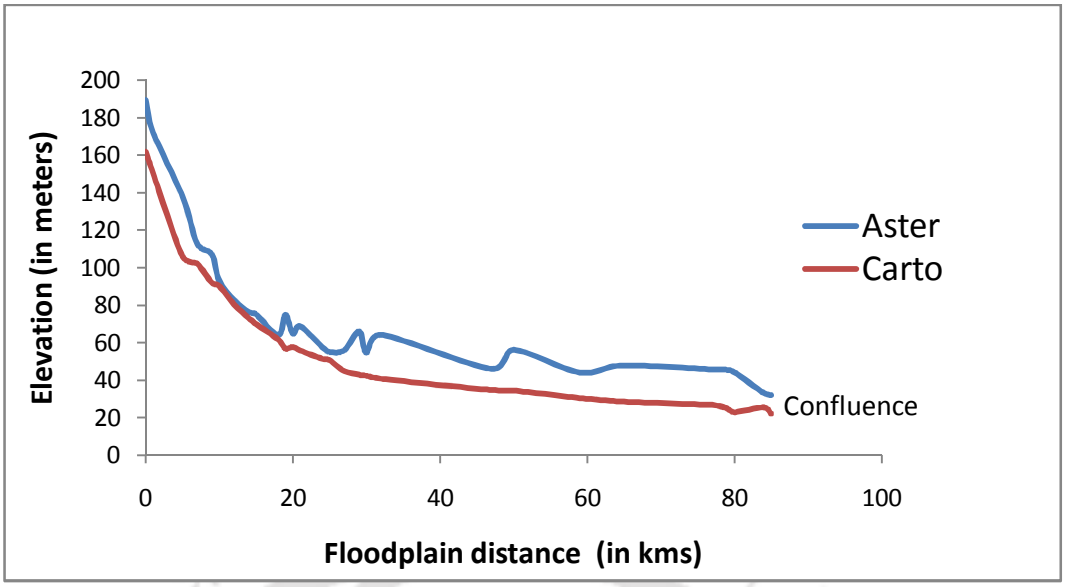

Fig.6.6: Extracted longitudinal profile of channel centreline of Pagladia

long river reach, almost throughout, ASTER derived bed profile is over estimating the CARTOSAT derived one by approximately 20 m. But it was satisfactory to see that both the profiles were maintaining a similar trend with an overall correlation of 0.974 as depicted in figure 6.7 below. Similarly in case of river Jiadhal, the same process has been performed. Figures 6.8 below reveal that ASTER derived river bed profile has

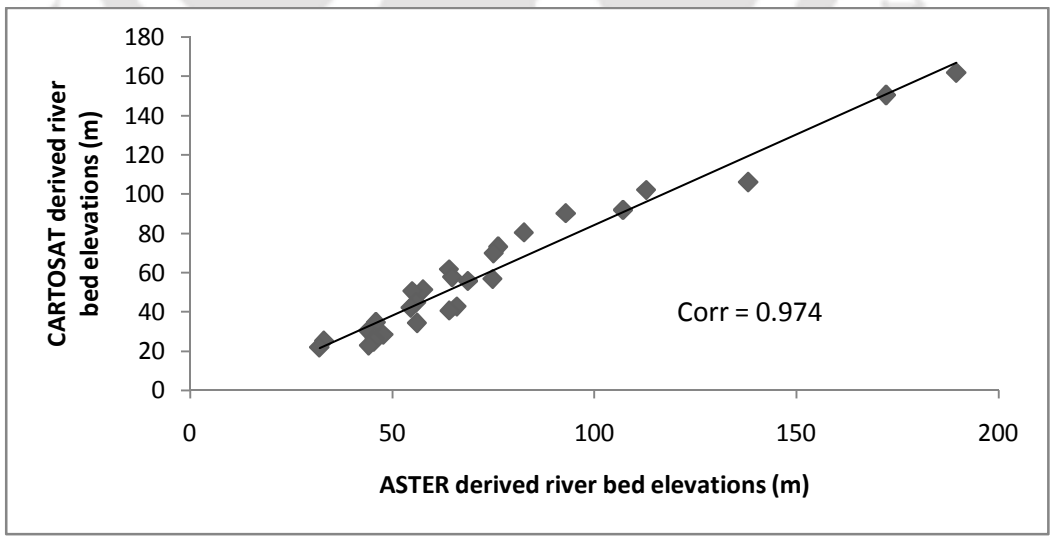

Fig.6.7: Bed profile correlation between ASTER and CARTOSAT in Pagladia

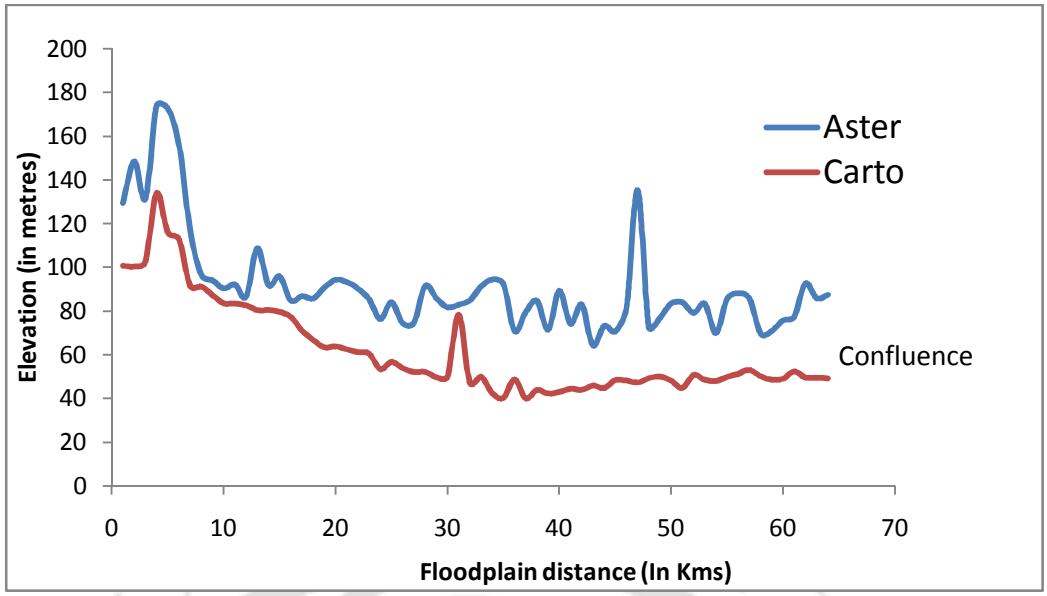

Fig.6.8: Extracted longitudinal profile of channel centreline in Jiadhal

once again over estimated the CARTOSAT derived bed profile by about 5 to 40 meters at various places along the 64 kms flood plain. Moreover both the bed profile generated

6.3.2 River cross section extraction

Traditionally channel geometry is collected in the field using different surveying techniques and tools. After establishing horizontal and vertical controls, elevations are taken along a cross-section. Collecting data in this manner is time consuming and costly. Recent development of satellite based survey techniques and popularity of GIS and photogrammetric techniques have opened an enormous possibility of extracting cross-section data from digital elevation models (DEMs). DEM and its role as cross-section data source is described in this section. In DEMs or DTMs the ground elevations are stored using formalized data structure rules such as Triangulated Irregular Network (TIN), or Grid. TINs can produce a more accurate representation of surfaces and features, but usually require a more extensive data collection effort. TINs represent surfaces as contiguous non overlapping triangular

faces. A surface value for any location can be estimated by interpolation of elevations within a triangle. Because elevations are irregularly sampled spatially in a TIN, this data structure allows a variable point density in areas where the terrain changes sharply, yielding an efficient and accurate surface model. Now the process of extracting cross-section data from a TIN involves defining the TIN as a surface and digitizing cross-section cutlines. A *cutline* represents the alignment of a cross-section in (x, y) or plan view. The ground elevation beneath each vertex is then interpolated from the surface. The elevations are either stored with the cross-section cutlines as 3-D lines or exported to a table. Figure 6.11 below shows a sample orientation of a cross section cutlines over

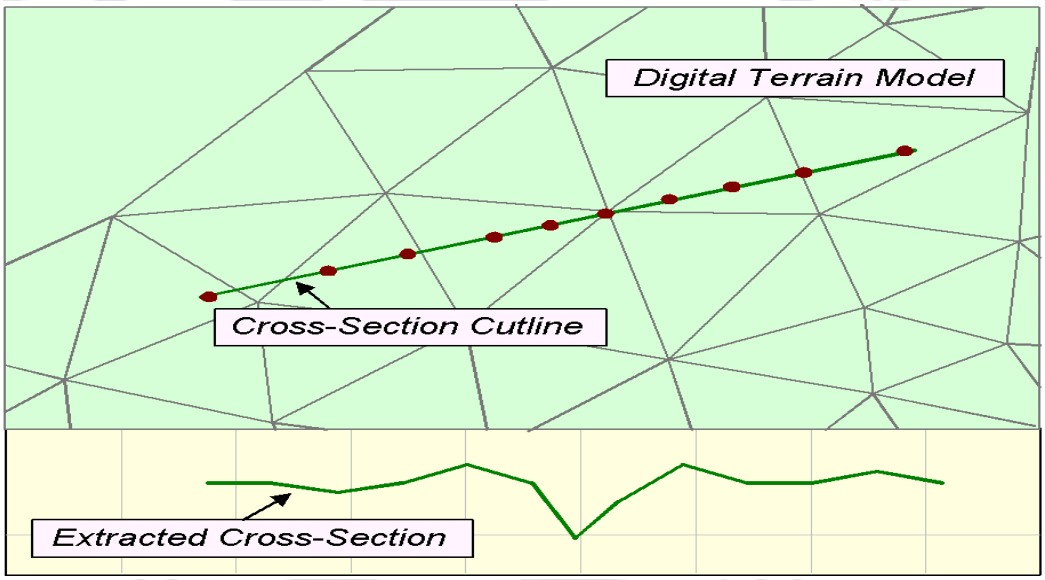

Fig. 6.11: Extraction of river cross section from DTM

a digital terrain model with the extracted cross section at the bottom. This process for extraction of cross sections in both Pagladia and Jiadhal rivers under the present study has been carried out in HEC Geo RAS platform. Here the cross sections are extracted in critical locations of the river channels using TIN developed from both the ASTER global DEM as well as the locally generated CARTOSAT-I stereo DEM. The xy cutline has always been kept perpendicular to the direction of flow

for extraction of these cross sections. Following figures shows the extracted cross sections in HEC-Geo RAS environment from ASTER and CARTOSAT-I stereo DEM.

Fig.6.12: A cross section in Pagladia upper reach by ASTER (left) and CARTOSAT-I (right)

The figure 6.12 above shows both the DEMs has yielded encouragingly similar cross sections at a location in the high altitude upper reaches of Pagladia river. Similarly cross sections were extracted for different locations of middle and the flood prone lower reach of the river also. Figure 6.13 below depicts the overall picture showing cross sections throughout the river reaches. Some of these extracted cross sections have

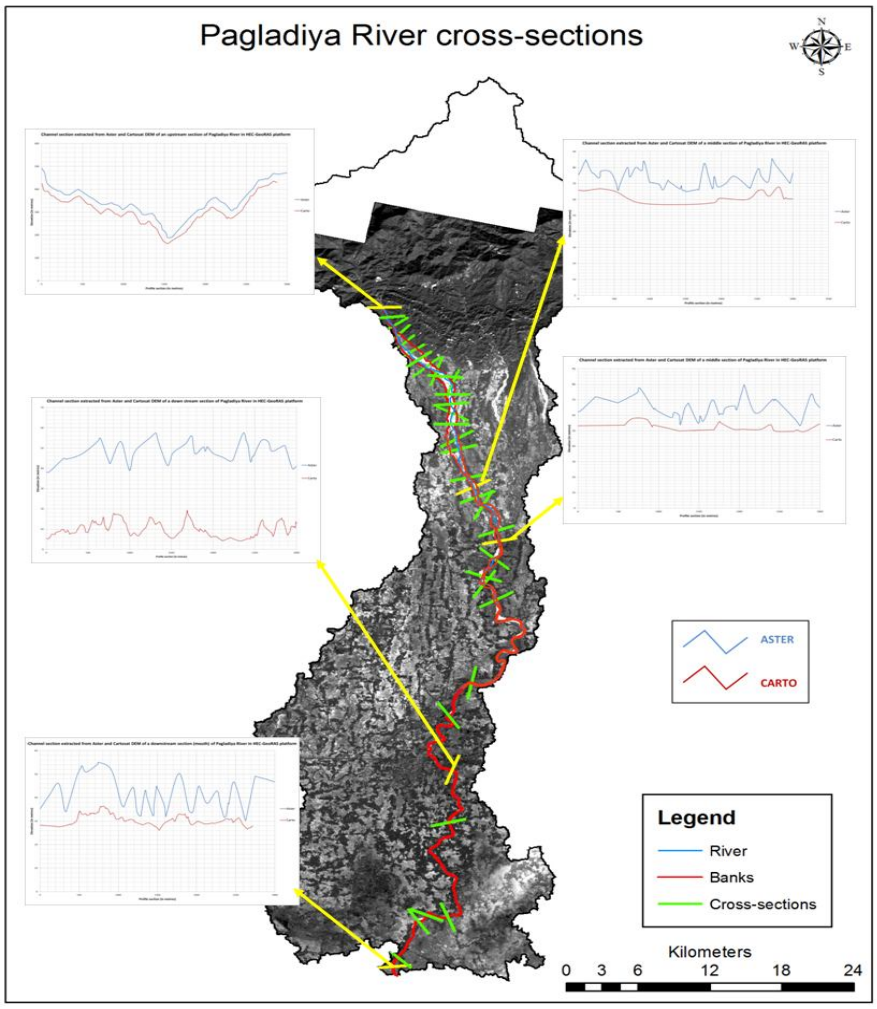

Fig. 6.13: Some of the cross sections extracted on Pagladia river

also been analyzed in greater detail in order to understand the relative merits and demerits of both the digital elevation models for extraction of cross sections in different altitudes such as upper, middle and lower reaches of Pagladia river. While surveying the literature available for the study area, hydrographical survey data of cross sections were found to be available (Source: Brahmaputra Board) for three location in upper middle, middle and lower reach of Pagladia river. Hence extracted cross sections in these locations namely Thalkuchi, N.T Road crossing and Brahmaputra outfall could be both graphically and statistically compared with these available ground survey data. Figure 6.14 below shows the comparison of both the ASTER derived and CARTOSAT – I derived cross section with the

hydrographically surveyed cross section data at Thalkuchi in the upper middle reach of Pagladia. Here the ASTER derived river cross

section has under estimated the hydrographically surveyed cross section by about 8 to

Like the previous river, in Jiadhal river also around fifteen plus cross sections have been extracted from both ASTER GDEM and the CARTOSAT – I stereo DEM. Out of them, three cross sections in critical locations where bathymetric data (Source: Brahmaputra Board) has been found to be available have been compared and analyzed

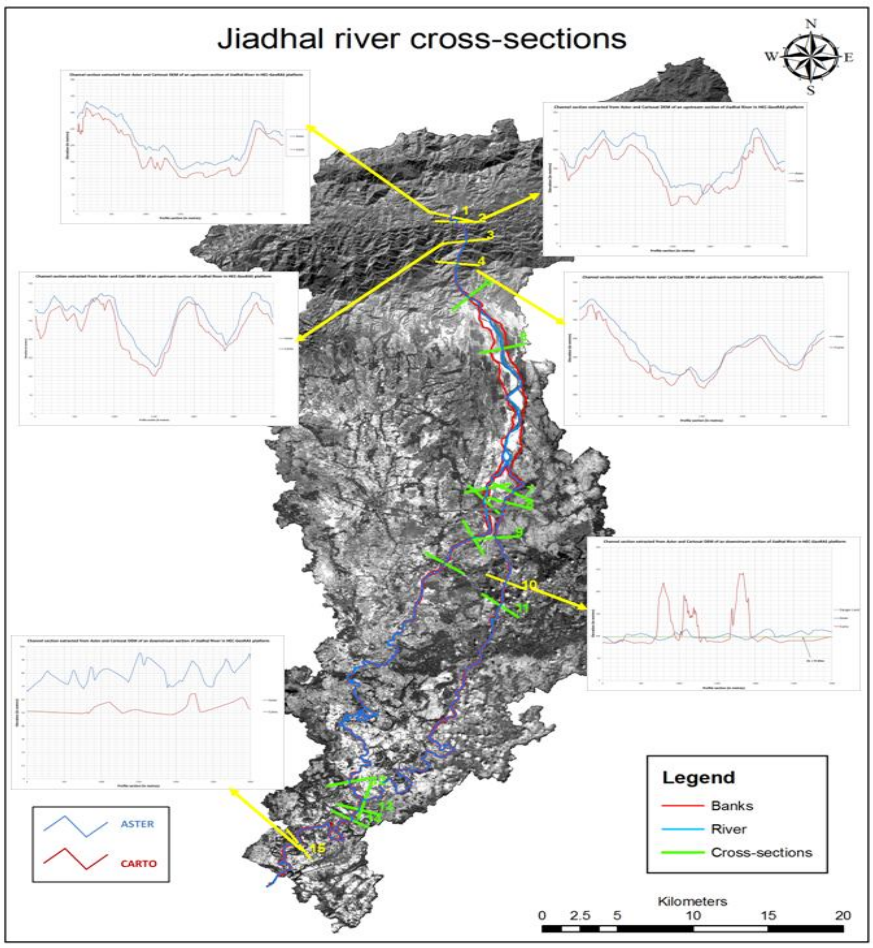

Fig. 6.18: Some of the cross sections extracted on Jiadhal river

for accuracy assessment. Figure 6.18 above has depicted the locations in the Jiadhal main river channel where cross sections have been extracted. Some of the cross sections where ground surveyed bathymetric data have not been available are

shown with extracted cross sections from ASTER and CARTOSAT –I. Three river sections located at places namely Jiadhalmukh on the upper middle reach, the Kumatia river confluence on the lower middle reach and the river outfall in lower reach were identified with available ground surveyed bathymetric data. As regard to the river cross section at Jiadhalmukh, it has been found that ASTER derived cross section has both overestimated and underestimated the ground surveyed bathymetry at different portions of floodplain profile section by about 20 to 50 meters as shown in figure 6.19 (a) above. Apart from difference in elevations, the trend across the floodplain has also been found to be conflicting supported by a rather poor correlation of 0.312 as depicted.

With this, the extracted cross sections in both the river channels under study, have been compared with ground survey data as available in both the river channels, where CARTOSAT –I stereo DEM has been found to extract more realistic river cross

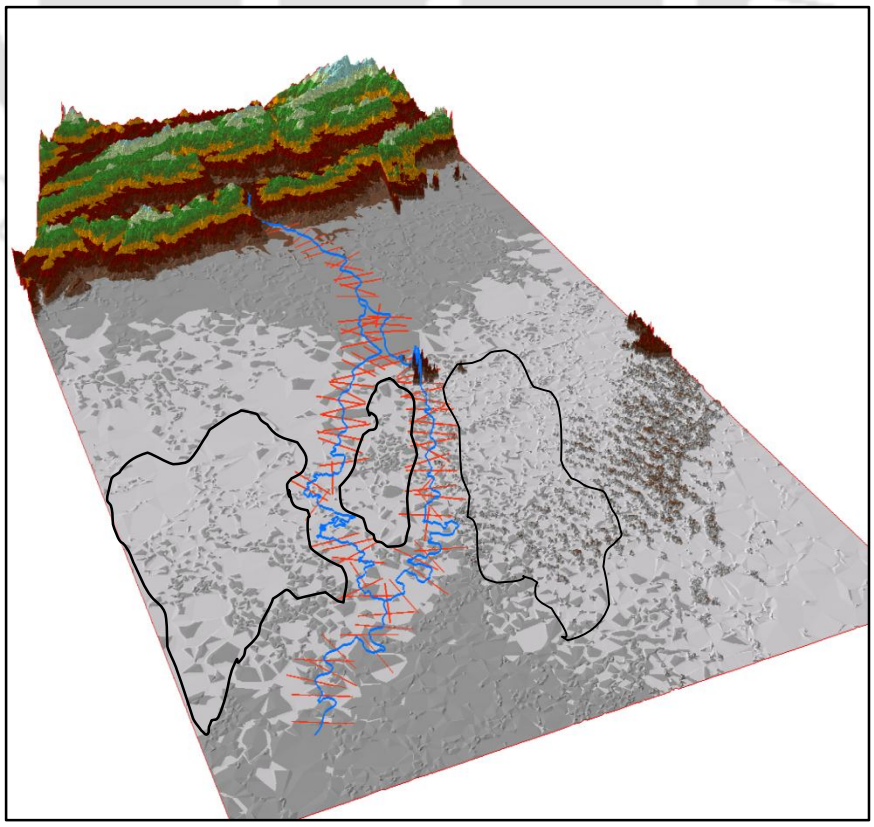

Fig. 6.22: Flooding zones in Jiadhal mid and lower reaches

sections (than that by the freely available ASTER global DEM) as a vital input for floodplain inundation modelling for flood hazard zonation.

6.4 COMPARISON OF RIVER BASIN HYPSOMETRY AS COMPUTED FROM ASTER GDEM AND CARTOSAT-I STEREO DEM

The river basin hypsometry essentially reveals how much of the basin occurs within what altitudinal range. Horton, 1932 and Strahler, 1952 did pioneering work on this area-altitude relationship in watershed scale. Langbein *et al.* 1947 extended the use of the hypsometric curve as a method of expressing slope and calculating mean altitude above the mouth of the basin. They reasoned the mean altitude above the mouth represented the potential head of a uniform depth of water over the basin and was a factor in the determination of the rate of accumulation of runoff. In addition they found a relationship between mean altitude above the mouth and the slope of the basin. All these studies in general have summarized that the hypsometric curve, a graphical representation of the area-elevation distribution in a basin, quantitatively describes geomorphic characteristics that have been shown to affect runoff. Further analysis of the hypsometric curve of a basin sheds additional light on the hydrograph of runoff from that basin. Hypsometry of a basin influences the time of concentration to the peak flow generation in a basin for a particular storm event. Thus an important input for flood forecasting. Sivapalan *et al.* 2003 have opined that hypsometry based perception for peak flow time becomes more important in ungauged basins where due to paucity of hydrological data, calibration of runoff models becomes difficult. Following this it was thought

to use DEM for hypsometric analysis of both the river basins for an overall understanding about the topographic distribution of the entire basin area.

6.4.1 Hypsometry of the Pagladia river basin

Both the ASTER GDEM and the CARTOSAT –I stereo DEM were classified as per the pixel wise elevation values (figure 6.4). Area under different elevation ranges

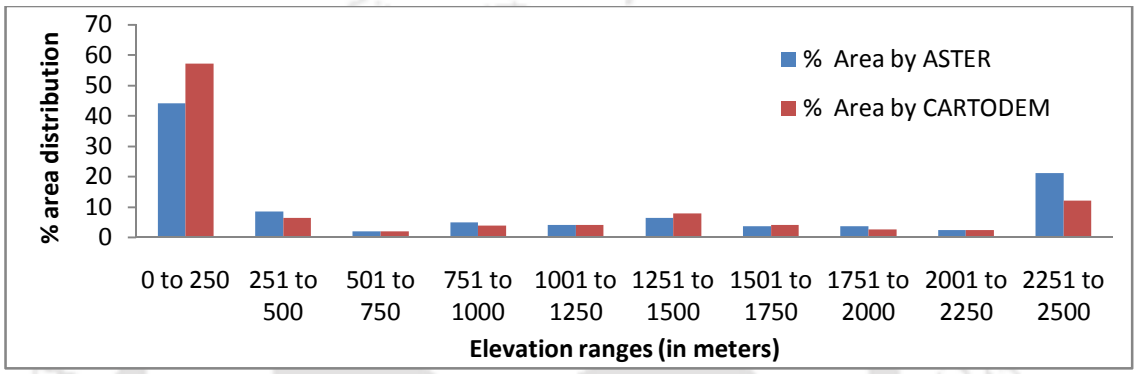

Fig. 6.23: Hypsometric plot of Pagladia basin

were identified and presented in percentage of the total available area of the basin as the hypsometric curve in figure 6.23 above. As per the developed hypsometric curve from the ASTER, around 44 % of the total area is occupied by the lower elevation ranges between 32 m to 250 m followed by around 21% by the highest altitudinal range between 2250 m and 2500 m. On the other hand the area distribution for these two altitude ranges in the hypsometry derived from the CARTOSAT – I DEM are around 57% and 12% respectively. Area distribution in mid altitude ranges as classified by both the DEMs are found to similar. Relatively small area in mid elevation ranges signifies lower time to peak flow generation. As far as relative performances are concerned, both ASTER and CARTOSAT – I DEMs have proven to be useful for hypsometric analysis. Minor differences in area calculation may be attributed to their varying capability to resolve minor vertical undulations.

6.4.2 Hypsometry of the Jiadhal river basin

Thematic classification of both the ASTER and the CARTOSAT- I DEM reveals the hypsometry of Jiadhal river basin as presented in figure 6.24 below.

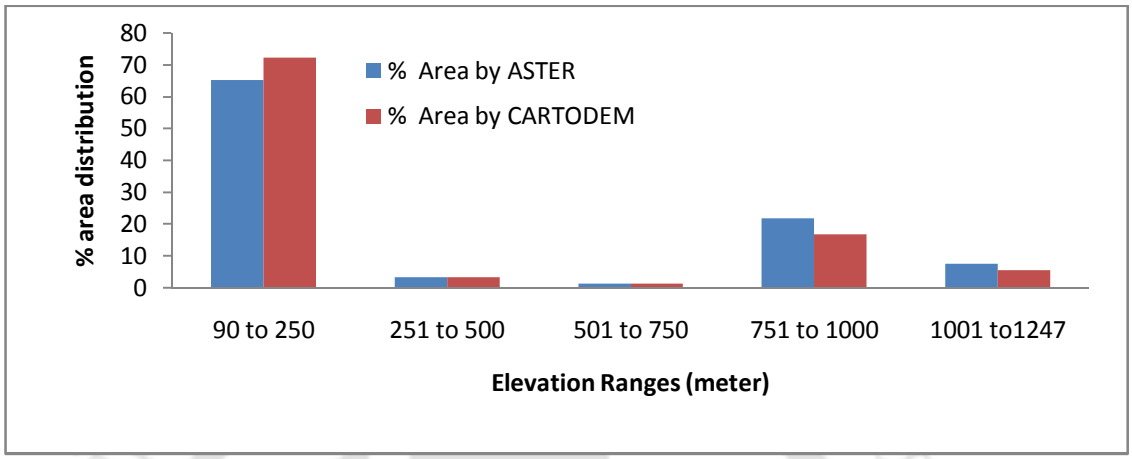

Fig. 6.24: Hypsometric plot of Jiadhal basin

Here the lowest range of elevations between 90 m to 250 m has been occupied by around 65% and 72% as classified by ASTER and CARTOSAT –I DEM respectively. Unlike the Pagladia river basin, here upper elevation ranges are occupied by around 28% of basin area between two ranges as per the ASTER DEM where as the area is around 23% as per the CARTOSAT – I DEM. But most interestingly the mid elevation range between 250m to 750 m has been shared among a very minimal percentage of area which is around 5% only as computed by both ASTER and the CARTOSAT – I DEM. This particular pattern of area distribution is responsible for flashy nature of overland flooding in Jiadhal river basin. Hence unlike Pagladia river where the hypsometry suggests a rather gentle build up of the peak flow, in Jiadhal basin the computed hypsometry suggests rapid peak flow formation which results flash floods making it relatively difficult to forecast flooding with actionable lead time.

In this chapter, the relative usefulness of a global freely available DEM and a locally generated stereo DEM for extraction of river cross section and basin

hypsometry has been studied. Significantly presence of cloud has been found to be a source of abrupt spikes in the cross section extracted from DEM. This source cannot be identified without having the ortho-rectified source data. Once it is conclusively known that these spikes are cloud induced, and then only they can be manually rectified. Another significant observation was that the bathymetry comparison with ground survey data sometimes also reveal horizontal shift of the channel. This has been observed and conclusively validated at the cross section at Thalkuchi in Pagladia river.

In this chapter basically the floodplain topography of the two river systems have been studied. In order to identify the degree of flood hazard associated with different parts of the floodplain, the topography hereby studied has been used as one of the parameter in a multi-criteria flood hazard evaluation exercise carried out in the next chapter of the present research work.

Chapter 7
FLOOD HAZARD ZONATION USING AN INNOVATIVE COMBINATION OF GEOSPATIAL AND MORPHOLOGICAL FIELD PARAMETERS

7.1 INTRODUCTION

The problem of riverine flooding is getting more and more acute due to human intervention in the flood plain (United Nations, 1976). Of late there is a realization that minimizing the risk and damage from floods may be a more rational way of flood management rather than simply formulating structural measures along the dynamic rivers. Flood hazard (probability of occurrence of a potentially damaging

phenomenon as stated by Varnes in 1984) mapping is one of the vital inputs for planning flood mitigation measures, and is a prerequisite for the community level flood insurance schemes. As flood itself cannot be prevented but the damages due to flood can be mitigated with proper planning and preparedness in community level, it is very important to identify the degree of hazard associated with various parts of a flood plain. Hence flood hazard zonation is an important component of overall flood management strategy. Different researchers across the globe have worked on various scientific and engineering techniques for identification of the degree of hazard associated with different parts of a floodplain. As mentioned in Chapter 2 earlier, plethora of these techniques may be classified in three broad categories and they are

(a) Flood hazard zonation based on existing historical records, inundation maps etc for a minimum of ten to fifteen year duration. Longer the duration better is the zonation.

(b) Zonation based on hydraulic flood inundation simulation and modelling.

(c) Zonation based on multi-criteria hazard evaluation

While the first two hazard zonation techniques have been developed up to a great extent with robust time series analysis and hydraulic simulations by different researchers (as reported in Chapter 2), the third category of hazard zonation techniques has been a relatively new area of research. Here, although the importance of floodplain geomorphology in flood hazard categorization has been reported way back in 1971 by Woolman, conclusive findings have started coming from the beginning of last decade onward. Researchers have used different combinations of parameters based on either causal geo-morphologic factors of flood or visible effect of historical flood on the surface of flood plain especially by

visualizing the floodplain through geospatial approaches such as satellite remote sensing indices. The example of using a judicious combination of both the remote sensing indices along with some geo-morphologic field parameters has been reviewed to be rather rare till date. Such a combination has been tried in the floodplains of these two tributaries under study and the exercise has been presented in this chapter.

Coming down to Pagladia lower reach, both the computed hazard zonations by RS indices and field parameters were satisfactorily validated (Figures 7.9 & 7.10) with actual inundation records, though here also the field parameters have performed relatively better than the RS indices. This better validation in lower reaches may be attributed to the presence of actual high inundation in a major portion of the floodplain.

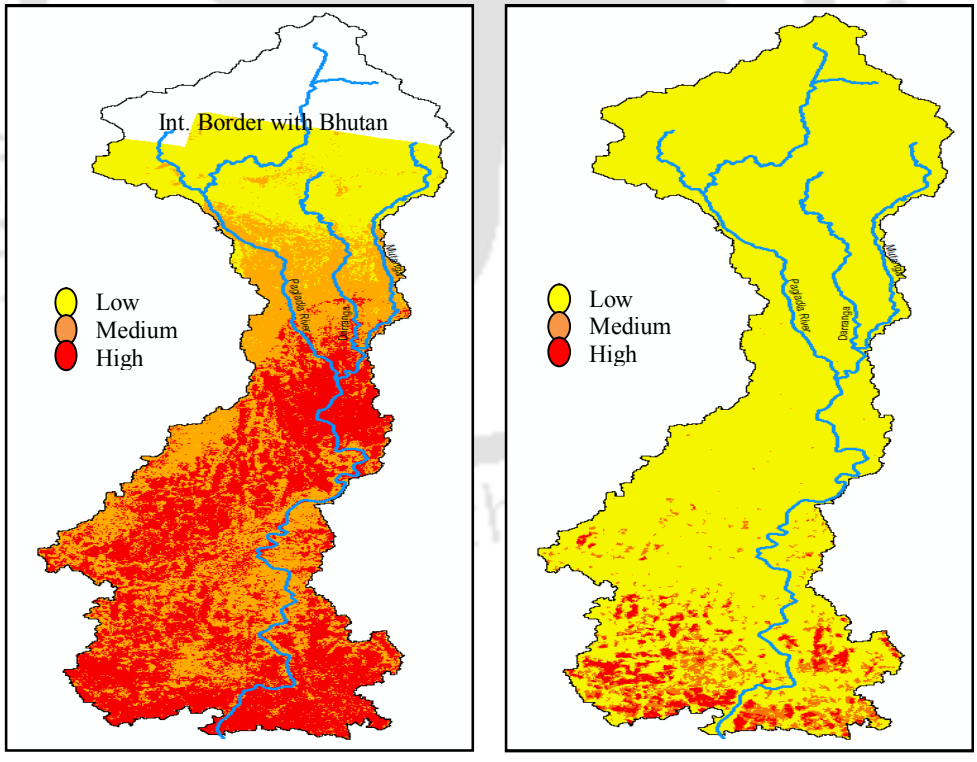

Figure 7.11: Computed FHZ by RS indices and field parameters combined (left) and the in situ inundation records (right) for the whole of Pagladia floodplain

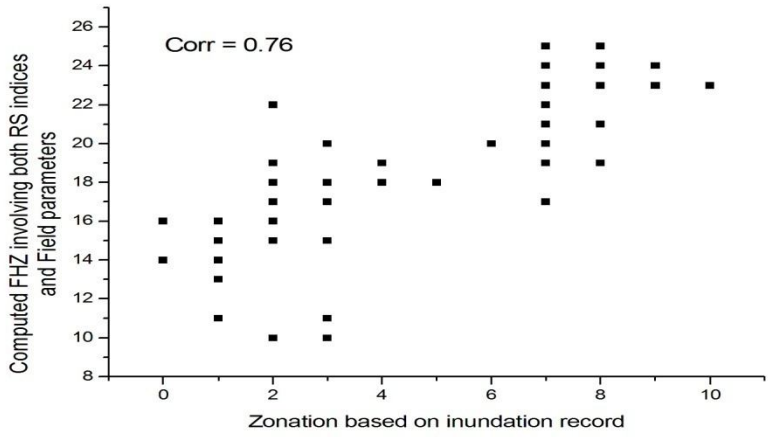

Figure 7.12: The correlation with all parameters combined for the entire floodplain of Pagladia river

Finally when the multi-criteria zonation was carried out combining both RS indices and the field parameters for the whole of the floodplain of Pagladia basin and validated against the same computed from actual flood inundation records, an encouraging correlation of 0.76 (Figure 7.12) was obtained.

7.5.2 Validation of flood hazard zonation in Jiadhal river basin

Just like the previous river basin, Jiadhal river floodplain has also been divided into middle and lower reaches. Similar processes that were followed for Pagladia basin for achieving data compatibility between the multi-criteria hazard zonation and the zonation from inundation records have been followed for Jiadhal river basin also. Like

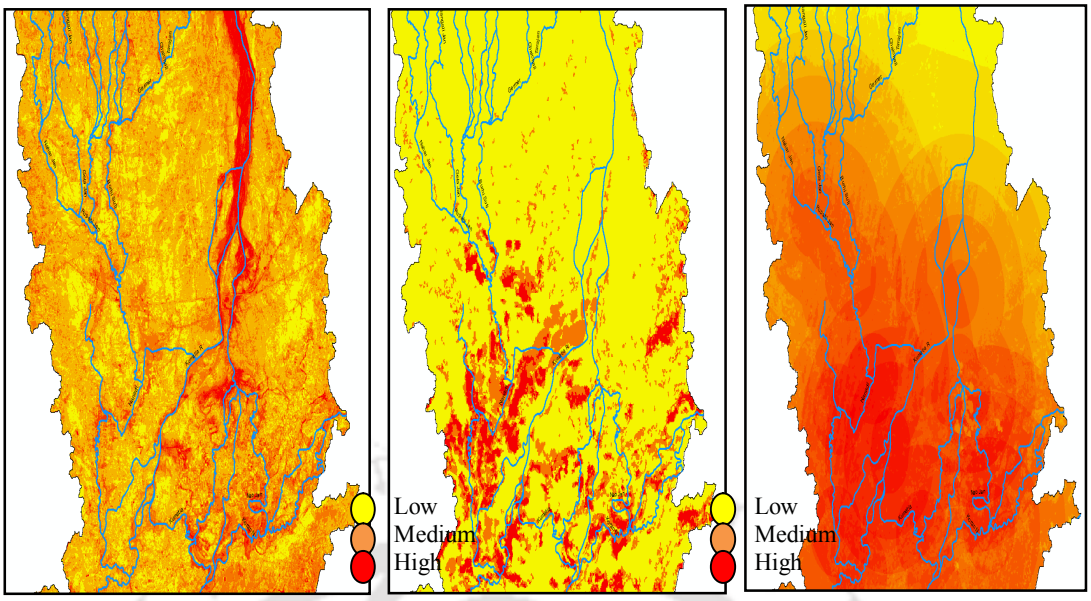

Figure 7.13: Computed FHZ by RS indices (left); in situ inundation record (Centre) and computed FHZ by field parameters (right) in Jiadhal middle reach

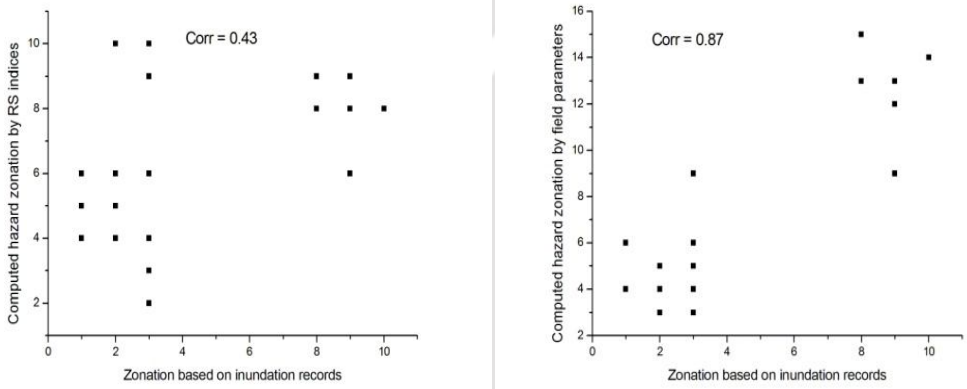

Figure 7.14: The correlations in Jiadhal middle reach

the case of Pagladia basin, here also the field parameters have been found to perform better then the RS indices. But even the RS indices have also performed relatively better than that in Pagladia middle reach. The reason may be attributed to the presence of good number of high hazard zones as per in situ inundation records. Among the field parameters, river confluence has proven to be influential in dragging the total weightage towards high hazard zones which have further tallied satisfactorily against the corresponding in situ inundation records. Now coming down to the lower reach of

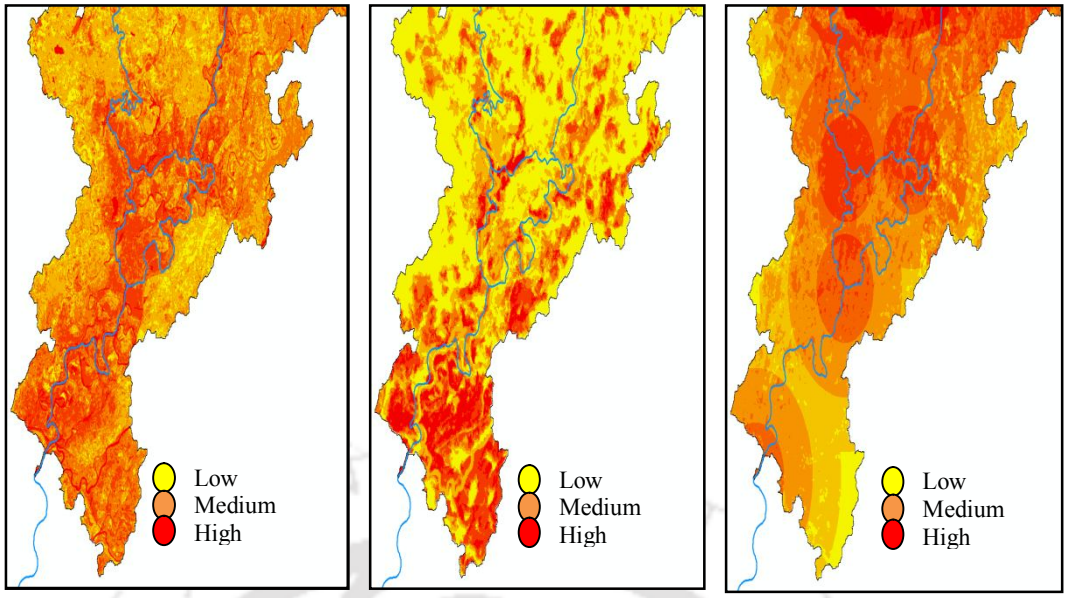

Figure 7.15: Computed FHZ by RS indices (left); in situ inundation record (Centre) and computed FHZ by field parameters (right) in Jiadhal lower reach

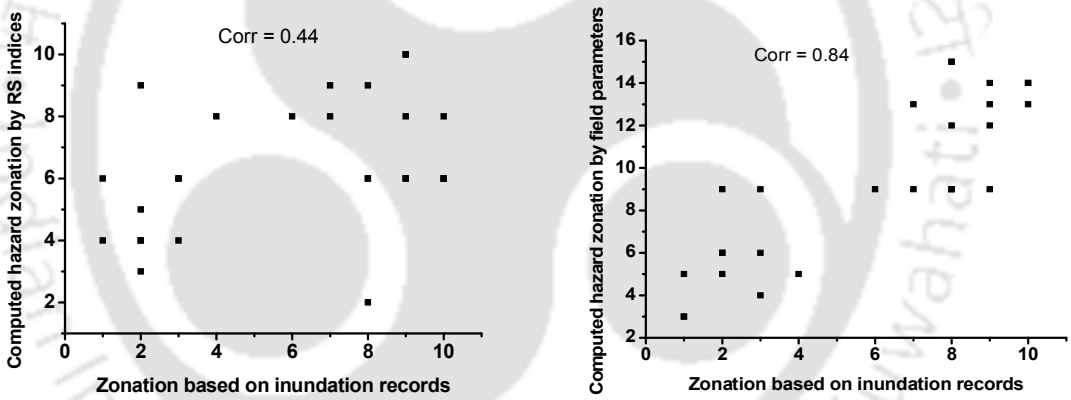

Figure 7.16: The correlations in Jiadhal lower reach

Jiadhal river, both the set of RS indices and field parameters have performed similarly as that of the middle reach with correlations of 0.44 and 0.84 respectively. The correctness of the selected hazard parameters based on effects of flood as well as causal factors of flood have been established here. Finally combining all the hazard

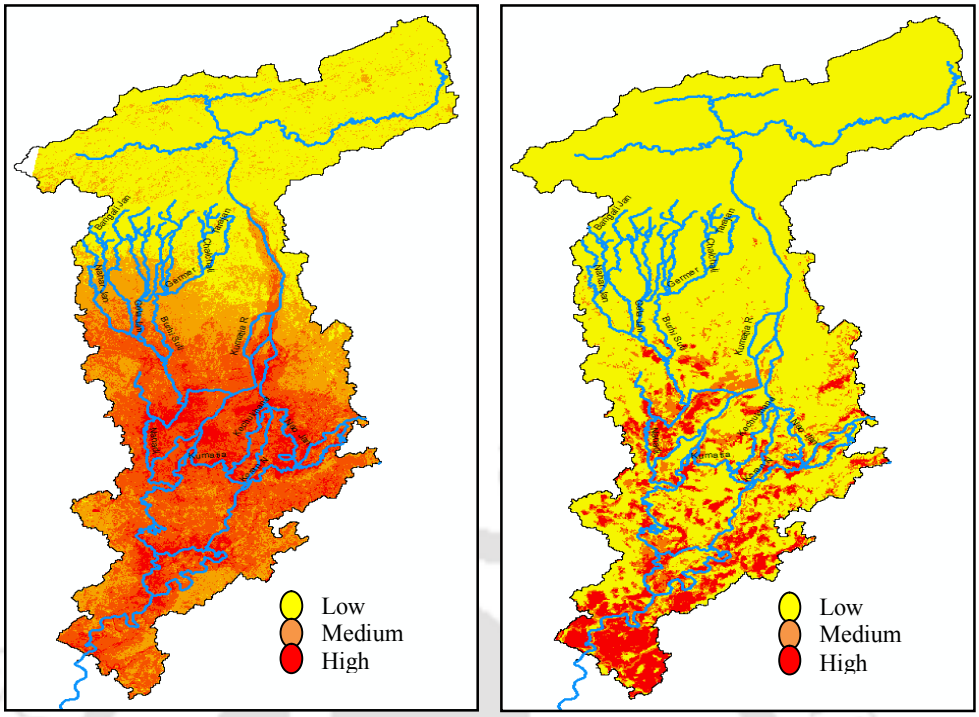

Figure 7.17: Computed FHZ by RS indices and field parameters combined (left) and the in situ inundation records (right) for the whole of Jiadhal basin

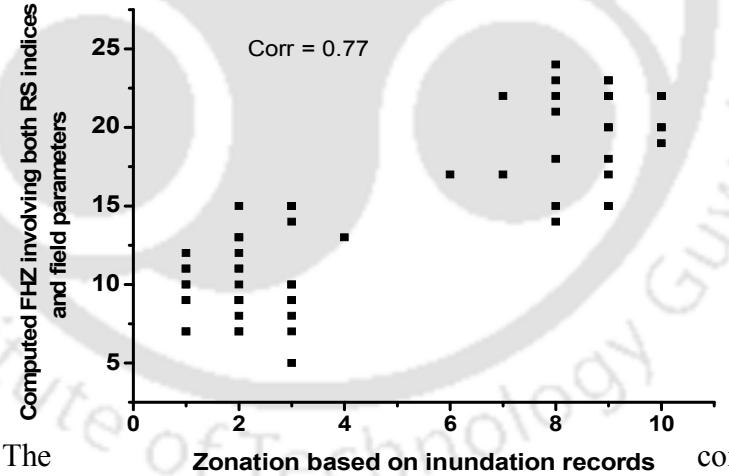

Figure 7.18: The correlation with all parameters combined for the entire floodplain of Jiadhal river

zonation parameters for the whole of the Jiadhal river floodplain (figure 7.17), a satisfactory correlation of 0.77 has been obtained when validated with in situ inundation records spanning over a period of 10 years as shown in figure 7.18.

After validation of this multi-criteria FHZ exercise in both the river floodplains under consideration, the field parameters based on the causal flooding

factors have been conclusively found to be more influential for correct identification of flood prone areas than the RS indices. RS indices have provided satisfactory results mostly in places of very frequent and severe flooding. But the field parameters have identified potential flooding areas even in non frequent flooding areas of middle reaches of both the floodplains. The combined effect of both the RS indices and the field parameters has also given satisfactory results when both the middle and lower reach were considered together. Thus this FHZ exercise has proven to be useful for floodplains with inadequately precise elevation information.

Chapter 8
SUMMARY AND CONCLUSION

8.1. INTRODUCTION

In this chapter the summarization of the major works performed pertaining to the objectives of the study followed by major conclusions have been presented. Scope for further extension of this research work has also been stated.

8.2. SUMMARY

Flood hazard management through non structural measures in developing and under developed countries is quiet inefficient and ineffective due to various factors like improper management of upper catchment areas, non availability of adequate number of hydro-meteorological surface observations, absence of techno-legal framework for floodplain regulation, lack of insurance provisions for floodplain dwellers among others. The present study aims to address some of these issues by studying the feasibility of application of geospatial tools for providing cost effective solutions for deriving some important input information for management of flood hazard.

8.2.1. On rainfall prediction by NWP techniques

It is well known that rainfall is the most vital input for forecasting of stream flow leading to early warning of flood. Proper on time recording of rainfall and its subsequent feeding into the run-off models is the key to the success of any flood forecasting system as a non structural measure for mitigation of flood damages. Moreover along with recording already occurred rainfall, prediction of an upcoming rainfall event correctly contributes immensely towards achieving actionable lead time of flood forecast. Review of literature has revealed that recent advances in weather study in geospatial domain have drastically changed the scenario mostly in technologically advanced countries. Two of these advances are RADAR measurement of occurring rainfall and Numerical Weather Prediction models for prediction of rainfall in different sizes of geographical domain and grid resolution. One such NWP technique known as the Weather Research Forecast (WRF) model has been tried and tested thoroughly during monsoon seasons in two flood prone river basins at different altitudes of the Brahmaputra valley in Assam, India within a nested domain covering major part of the Brahmaputra valley at 9 kilometre gridded resolution. Input data of wind speed, wind direction, temperature, pressure, relative humidity were assimilated from the global platform of NASA GFS for the first monsoon season in 2011 and from locally installed AWS for the second season in 2012. Six rainfall events each month for three peak monsoon months of June, July and August were considered for both the years. The predicted rainfall values were validated against global RADAR rainfall measurements under TRMM as well as in situ rainfall recorded by AWS installed locally in both the basin.

8.2.2. On usability of WRF rainfall prediction as input in stream flow prediction

Along with the storm characteristics, static characteristics of river basin such as size, shape, slope, soil, land use etc also play vital role in hydrologic response of a basin to a particular rainfall event. In order to compute flood discharge from the rainfall values predicted by the WRF numerical weather prediction model, two runoff modelling approaches were adopted. One of them was rather simple and well known lumped model known as the rational formula and the other was the distributed HEC-HMS model. GIS platform was used to generate all the important input layers such as watershed boundary, land use, soil map, DEM, drainage and confluence etc for building these models. While the rational formula yielded the peak discharge (with an assumption that rainfall was spatio-temporally uniform throughout the time of concentration for both the basin and it is worth mentioning that the TOC for Pagladia and Jiadhal basin were calculated to be 21 hours and 18 hours respectively with the Kirpich formula), the HEC-HMS yielded the daily hydro-graph at basin outlet locations. As both the river basins were devoid of any real time discharge data in the designated hydro observation sites, the computed flood peak by rational formula and the peak of the 24 hourly hydrograph had to be validated indirectly against available daily stage data in both the river basins. The computed peaks were further compared with some available historical flood frequency information only to examine the legitimacy of the computed flood peaks for the concerned river basins.

8.2.3. On extraction of river hydraulic geometry from DEM

Once the flood discharge is predicted at a particular point in a river basin, the next issue that arises is regarding the spread of flood inundation in the floodplain corresponding to the predicted discharge or stage. Floodplain hydraulic geometry is one of the most vital input for two dimensional simulation of flood inundation. With the advancement of geospatial techniques, Digital Elevation Models are

widely used for extraction of river hydraulic profile (both longitudinal and cross-section). Due to easy availability in public domain, online global DEMs such as SRTM, GTOPO, ASTER etc. are popular choices among researchers. Literature review has revealed the limitations of these global DEMs for extraction of topography of flat alluvial terrain. Some researchers in the recent past have opined about relative capability of these DEMs for extraction of river and floodplain hydraulic geometry. DEMs generated through photogrammetric techniques using a pairs of stereo images are known to yield better vertical accuracy and has been used for topographic mapping on a local scale. A pair of single band stereo images from an Indian optical sensor CARTOSAT-I with spatial resolution of 2.5 metre has been processed in LPS photogrammetric software to generate the DEM for both the river basins under study. Similarly both the river basins were also carved out from the ASTER global DEM. Both these two different DEMs were processed in HEC Geo-RAS platform for extraction of the river geometry (both longitudinal profile and cross-sections) in some prime locations of their floodplains. Moreover both the different DEMs were also analysed for basin hypsometry. River geometry extracted from both the DEMs were compared with available ground surveyed river geometry data.

8.2.4. On multi-criteria flood hazard zonation (FHZ) based on Remote sensing indices and morphologic field parameters

Apart from hydraulic simulation of flood inundation extent, identification of flood hazard zones based on probability of flood occurrence is also a vital information for medium to long term flood hazard management planning. In order to achieve preparedness at community level, identification of the degree of hazard associated with different parts of the floodplain is of paramount importance. These hazard zones are generally identified either by complicated two dimensional hydraulic

simulation supported by extremely precise topographic information or by time series analysis of historical inundation maps for long durations without data gaps. Literature review has suggested a third newer approach which is based on presence or absence of favourable flooding genesis over the river basin concerned. Some of these factors are morphological field parameters across the floodplain and the apparent effect of frequent flooding on the surface of the floodplain. Getting inspired from some of the works carries out by researchers during the last decade, a multi-criteria weightage based decision analysis was tried for identifying different degrees of hazard associated with different part of the floodplains of both the river basins under study. Two remote sensing indices namely the Normalised Difference Vegetation Index (NDVI) and the Normalised Difference Moisture Index (NDMI) were used in combination as the first approach of hazard zonation followed by the second approach involving three field floodplain specific parameters such as the elevation, proximity to river confluences and proximity to embankment breaches. While the first approach is based on effects of frequent flooding on floodplain the second one is based on some common causal factors for flooding in alluvial river valleys. The identified hazard zones by the first approach alone, by the second approach alone and by the combination of both were tested separately against 10 years of satellite derived inundation records available as district wise atlas covering the floodplains of both the rivers.

References

Anthes, R.A, Warner, T.T. (1978), "Development of hydrodynamic models suitable for meso-meteorological studies." Bulletin of American Meteorological Society, 106, p. 1045 – 1078.

ATLAS volume 1996, Master Plan of Pagladia Sub-basin, Brahmaputra Board, Ministry of Water Resources, Govt. of India, Plate 24.

Ahrens, S.R. and Maidment, D.R. (1999), "Flood forecasting for the buffalo bayou using CRWR-PrePro and HEC-HMS." CRWR report, 1999, Austin, Texas.

ATLAS volume 2000, Master Plan of Jiadhal Sub-basin, Brahmaputra Board, Ministry of Water Resources, Govt. of India, Plate 13.

Anderson, M.L., Chen, Z.Q., Kavvas, M.L. and Feldman, A. (2002), "Coupling HEC-HMS with atmospheric models for prediction of watershed runoff." Journal of Hydrologic Engineering, 7, p. 312 – 318.

Abrams, M., Hook, S, Ramachandran, B. (2002), "ASTER User Handbook, Version 2."
http://asterweb.jpl.nasa.gov/content/03_data/04_Documents/aster_user_guide_v2.pdf, retrieved May 2006.

Agirre, U., Goni, M., Lopez, J.J., Gimena, F.N. (2005), "Application of unit hydrograph based on subwatershed division and comparison with Nash's instantaneous unit hydrograph." CATENA, 64, p. 321 – 332.

Akter, N. and Islum, M.N. (2007), "Use of MM5 model for weather forecasting over Bangladesh region." BRAC University Journal, 4, p. 75 - 79.

Aguilar, F.J., Mills, J.P., Delgado, J., Aguilar, M.A., Nagreiros, J.G., Perez, J.L. (2010), "Modelling vertical error in LIDAR derived Digital Elevation Models." ISPRS Journal of Photogrammetry and Remote Sensing, 65, p. 103 – 110.

Battan, L.J. (1973). "Radar observation of the atmosphere." The university of Chicago press, pp 324.

Bevan, K.J., Kirkby, M.J. (1979), "A physically based variable contributing area model of basin hydrology." Hydrological Science Bulletin, 24, p. 43 – 69.

Bruneau, P., Gascuel-Odoux, C., Robin, P., Merot, P.H., Beven, K. J. (1995), "Sensitivity to space and time resolution of a hydrological model using digital elevation data." Journal of Hydrological Processes, 9, p. 69 – 82.

Bloschl, G., Sivapalan, M. (1995), "Scale issues in Hydrological modelling: A review." Journal of Hydrological Processes, 9, p. 251 – 290.

Bedient, P.B., Holder, A., Benavides, J.A., Vieux, B.E. (2003), "Radar- Based Flood Warning System Applied to Tropical Storm Allison." Journal of Hydrologic Engineering, 8 (6), p. 308-318.

Bao, Z., Jianyun, Z., Jiufu, L., Guoqing, W., Guobin, F., Ruimin, H., Xiaolin, Y. (2011), "Estimation of base flow parameters in variable infiltration capacity model using soil properties." Journal of Advances in Water Science, 53, p. 63 – 71.

Bhatt, C.M., Rao, G.S., Manjusree, P., Bhanumurthy, V. (2011), "Potential for high resolution satellite data for disaster management: A case study of Leh, Jammu & Kashmir (India) flash flood, 2010." Journal of Geomatics, Natural Hazards and risk, 2, p. 365 – 375.

Charney, J.G., Elliassen, A. (1949), "A numerical method of Predicting the perturbations of the middle latitude westerlies." Journal of life sciences/ Meteorology, 1, p. 38 – 54.

Clarke, J.I. (1966), "Morphometry from Maps. Essays in Geomorphology." Elsevier Publication, New York, p. 235 - 274.

Cavallini, F. (1993), "Computing the unit hydrograph via linear programming." Journal of Computers and Geosciences, 19, p. 1285 – 1294.

Carpenter, R.L.J., Droegmeier, K.K., Bassett, G.M., Weygandt, S.S., Jahn, D.E., Stevenson, S., Qualley, W., Strasser, R. (1999), "Storm scale numerical weather prediction for commercial and military aviation. Part I: Results from operational tests in 1998." Conf. on Aviation, Range and Aerospace, American Meteorological Society., p. 209 – 211.

Chen, P., Chin, S., Lim, H. (1999), "Flood Detection using Multi-temporal Radarsat and ERS SAR data." http://www.gisdevelopment.net/aars/acrs/1999/p.56.

Carlos, A., Forero, V., Torres, D.S., Cassiraga, E.F., Harnandez, J.J.G. (2009), "A non parametric automatic blending methodology to estimate rainfall fields from rain gauge and radar data." Journal of Advances in Water Resources, 32, p. 986 – 1002.

Doviak, R. J., and Zrnic, D.S. (1993), "*Doppler Radar and Weather Observations.*" Academic Press, p.562.

Duan, Q., Gupta, V.K., Sorooshian, S. (1993), "A shuffled complex evolution approach for effective global minimization." Journal of Optimization theory and applications, 76, p. 501 – 521.

Droegemeier, K.K (1997), "The numerical prediction of thunderstorms: Challenges, potential benefits and results from real time operational tests." Bulletin of World Meteorological Organization, 46, p. 324 – 336.

Devi, H.I. (2000), "Drainage Morphometry (Chapter 2)" The book: River Basin Morphology, Rajesh Publications, New Delhi, p. 21.

Datta, B., Singh, V.P. (2004), "Hydrology (Chapter 8)" The book: Brahmaputra Basin Water Resources, Kluwer Academic Publisher of Netherland, p. 139 – 195.

Dyhouse, G., Hatchett, J. (2005), "Flood modelling using HEC-RAS" Vol 2, Haestad press publications.

DeAlwis, D. A., Easton, Z. M., Dahlke, H. E., Philpot, W. D., Steenhuis, T. S. (2007), "Unsupervised classification of saturated areas using a time series of remotely sensed images." Journal of Hydrology and Earth System Sciences, 4, p. 1663–1696.

EL- Sammany, M.S. (2010). "Forecasting of Flash Floods over WadiWatier – Sinai Peninsula Using the Weather Research and Forecasting (WRF) model." Journal of World Academy of Science, Engineering and Technology, 46, p. 996-1000.

Franchini, M., Wendling, J., Obled, C., Todini, E. (1996), "Physical interpretation and the sensitivity analysis of the TOPMODEL." Journal of Hydrology, 175, p. 293 – 338.

Feldman, A.D. (2000), Hydrologic Modelling System HEC-HMS: Technical Reference Manual.

Fraser, C.S., Baltsavias, E., Gruen, A. (2002), "Processing of IKONOS imagery for sub meter 3D positioning and building extraction." ISPRS Journal of Photogrammetry and Remote Sensing, 56, p. 177 – 194.

Falorni, G., Teles, V., Vivoni, E.R., Bras, R.L., Amaratunga, K.S. (2005), "Analysis and characterization of vertical accuracy of digital elevation models from Shuttle Radar Topography Mission." Journal of Geo-physical Research, 110, F02005.

Goswami, D. C. (1985), "Brahmaputra River, Assam, India: physiography, basin denudation, and channel aggredation." Journal of Water Resource Research, 21, p. 959 - 978.

Garrote, L., Bras, R.L. (1995), "A distributed model for real-time flood forecasting using digital elevation models." Journal of Hydrology, 167, p. 279 – 306.

Goswami, D.C. (1998), "Fluvial regime and flood hydrology of Brahmaputra river, Assam." Bulletin of Geological society of India, 41, p. 53 – 75.

Gosain, A.K., Rao, S., Srinivasan, R., Reddy, N.G. (2005), "Return flow assessment for irrigation command in the Palleru river basin using SWAT model." Journal of Hydrological Processes, 19, p. 673 – 682.

Gorochovich, Y., Voustianiouk, A. (2006), "Accuracy assessment of the processed SRTM-based elevation data by CGIAR using field data from USA and Thailand and its relation to the terrain characteristics." Journal of Remote Sensing of Environment, 109, p. 409 – 415.

Gichamo, T.Z., Popescu, I., Jonoski, A., Solomatine, D. (2011), "River cross section extraction from ASTER global DEM for flood modelling." Journal of Environmental Modeling and Software, 31, p. 37 – 46.

Horton, R.E. (1932), "Drainage basin Characteristics." Transactions, American Geo-physical union, 13, p. 350 – 361.

Horritt, M.S., Bates, P.D. (2001), "Predicting flood plain inundation: Raster based modelling versus finite element approach." Journal of Hydrological Processes, 15, p. 825 – 842.

Horritt, M.S., Bates, P.D. (2002), "Evaluation of 1 D and 2 D numerical models for prediction of flood inundation." Journal of Hydrology, 268, p. 87 – 99.

Hirano, A., Welch, R., Lang, H. (2003), "Mapping from ASTER stereo image data: DEM validation and accuracy assessment." International Journal of Photogrammetry and Remote Sensing, 57, p. 356 – 370.

http://www.hec.usace, "A single event rainfall runoff hydrologic model (Chapter 6)." User Manual, Version 3 (2005), p. 104.

Hayes, D.C., Young, R.L. (2006), "Comparison of peak discharge and runoff characteristics estimates from the Rational Method to field observations for small basins in central Virginia: U.S.G.S scientific investigations report." p. 38.

Ho, L.T.K., Umitsu, M., Yamaguchi, Y. (2010), "Flood hazard mapping by satellite images and SRTM DEM in the VU GIA – THU BON alluvial plain, Central Vietnam." Int. Archive of Photogrammetry, Remote Sensing and Spatial information science, XXXVIII, p. 275 – 280.

Ide, K., Courtier, P., Ghil, M., Lorenc, A. C. (1997), "Unified notation for data assimilation: Operational, sequential and variational." Journal of Meteorological Society of Japan, 75, p. 181–189.

Jain, S., Lal, U. (2001), "Floods in changing climate: Does the past represent the future?" Journal of Water Resources Research, 37, p. 3193 – 3205.

Jacobsen, K. (2001), "New developments in Digital Elevation Modelling." Journal of Geoinformatics, June,2001, p. 18 – 21.

Jayakrishnan, R., Srinivasan, R., and Arnold, J.G.(2004), "Comparison of rain gauge and WSR–88D Stage III precipitation data over the Texas-Gulf Basin." Journal of Hydrology, 292, p. 135–152.

Jha, M., Pan, Z., Takle, E.S., Gu, R. (2004), “Impact of climate change on stream flow in the upper Mississippi river basin.” Journal of Geophysical Research, 109, p. 1 – 12.

Jain, S.K., Singh, R. D., Jain, M. K., Lohani, A. K. (2005), “Delineation of Flood-Prone Areas Using Remote Sensing Techniques.” Journal of Water Resources Management, 19, p. 333–347.

Johnson, B.H., Padmanabhan, G. (2010), “Regression estimates of design flows for ungauged sites using bankful geometry and flashiness.” CATENA, 81, p. 117 – 125.

Kuichling, E. (1889), “The relation between the rainfall and the discharge of sewers in Populous districts.” Transactions, American Society of Civil Engineers, 20, p. 1–56.

Klemp, J. B., Wilhelmson, R.(1978), “The simulation of three-dimensional convective storm dynamics.” Journal of Atmospheric Science, 35, p. 1070–1096.

Lilly, D.K. (1983), "Stratified turbulence and the meso scale variability of the atmosphere." Bulletin of American meteorological society, 132, p. 749 - 761.

Kamp, U., Bolch, T., Olsenholler, J. (2003), “DEM generation from ASTER satellite data for geomorphic analysis of Cerro Sillajhuay, Bolivia.” Proc. Of ASPRS annual conference, Anchorage, Alaska.

Knebl, M.R., Yang, Z.L., Hutchison, K., Maidment, D.R. (2005), “Regional scale flood modelling using NEXRAD rainfall, GIS and HEC-HMS/RAS: A case study for the San Antonio river basin summer 2002 storm event.” Journal of Environmental Management, 75, p. 325 – 336.

Klemp, J. B., Skamarock, W. C., Dudhia, J. (2007), “Conservative split-explicit time integration methods for compressible non-hydrostatic equations.” Mon. Wea. Rev., 135, p. 2897 – 2913.

Kashid, S.S., Gupta, K. (2010), "Hydrological and hydraulic modelling of river Sabarmati stretch in Ahmedabad using HEC-HMS and HEC-RAS respectively." Water and Energy international, 67, p. 67 – 71.

Langbein, W.B., Basil, W. (1947), "Topographic characteristics of drainage basins." USGS water supply paper, 947 – c.

Laprise R. (1992), "The Euler Equations of motion with hydrostatic pressure as as independent variable." Mon. Wea. Rev., 120, P. 197–207.

Liang, X., Wood, E.F., Lettenmaier, D.P. (1996), "Surface soil moisture parameterization of the VIC-2L model: Evaluation and modification." Journal of Global and Planetary change, 13, p. 195 – 206.

Lutes, J. (2006), "First impressions of CARTOSAT – I." In: JACIE Civil and Commercial imagery evaluation workshop, Laurel, Maryland, March 14 – 16, 2006.

Lastra, J., Fernandez, E., Herrero, D., Marquinez, J. (2008), "Flood hazard delineation combining geomorphological and hydrological methods: an example in the northern Iberian peninsula." Journal of Natural Hazards, 45, p. 277 – 293.

Middleton, W.E.K. and Spilhaus, A.F. (1953) "Meteorological instruments", 3rd edition, University of Toronto press.

Moore, I. D., Grayson, R. B., Ladson, A. R. (1991), "Digital terrain modelling: A review of hydrological, geomorphological, and biological applications." Journal of Hydrological Processes, 5, p. 3–30.

Mack, M.J. (1995), "HER – Hydrologic Evaluation of Run-off; the soil conservation services curve number technique as an interactive computer model." Journal of Computers and Geosciences, 21, p. 929 – 935.

McFeeters, S.K. (1996), "The use of Normalised Difference Water Index (NDWI) in the delineation of open water features." International Journal of Remote Sensing, 17, p. 1425 – 1432.

Master Plan of Jiadhal Sub-basin, Report volume 2000, Brahmaputra Board, Ministry of Water Resources, Govt. of India, Chapter 1, p. 1.

Mongkolsawat C .,Thirangoon P., Suwanwerakamtorn R., Karladee N., and Paiboonsak S. (2003), "Evaluating Flood Risk Area using GIS and RADARSAT Data- A Case Study in Northeast Thailand." Proc. of Asian Conf. of Remote Sensing, Pusan.

Mishra, S.K., Singh, V.P. (2003), "Soil conservation services curve number (SCS-CN) methodology." Kluwer academic publisher, p. 480.

Murthy, Y.V.N.K., Rao, S.S., Rao, D.S.P., Jayaraman, V. (2008), "Analysis of DEM generated by CARTOSAT-I stereo data over MUSSANE LES ALPILES." International archive of Photogrammetry, Remote sensing and spatial information, XXXVII, p. 1343 – 1348.

Moustafa, S., Sammany, E.L. (2010), "Forecasting of Flash Floods Over Wadi Watier – Sinai Peninsula Using the Weather Research and Forecasting (WRF) Model." Jounal of Nile basin water science and Engineering, 3, p. 88 – 95.

Maussion, F., Scherer, D., Finkelnburg, R., Richters, J., Yang, W., Yao, T. (2011). "WRF simulation of a precipitation event over the Tibetal plateau, China – An assessment using remote sensing and ground observation." Journal of Hydrology and Earth System Sciences, 15, p. 1795 – 1817.

Mishra, A. (2012), "Estimation of heavy rainfall during cyclonic storm from microwave observation using non linear approach over Indian ocean." Journal of Natural Hazards, doi: 10.1007/s 11069-012-0179-4.

Mujumdar, P.P., Kumar, D.N. (2013), "Part- III: Remote Sensing, GIS and DEM for modeling of floods." of the book "Floods in changing climate: Hydrologic Modeling" International Hydrology Series, ISBN-9781107018761.

Ooyama, K. V. (1990), "A thermodynamic foundation for modelling the moist atmosphere." Journal of Atmospheric Sciences, 47, p. 2580–2593.

Oya, M. (2002), "Applied geomorphology for mitigation of natural hazards." Journal of Natural Hazards, 25, p.17-25.

Patil, J. P., Sarangi, A., Singh, O. P., Singh, A. K., Ahmad, T. (2008). "Development of a GIS Interface for estimation of runoff from watersheds." Journal of Water Resources Management, 22, p. 1221 - 1239.

Richardson, L.F. (1922), "Weather predictions by numerical processes (2nd Edition)" , Cambridge University Press.

Riggs, H.C. (1985), "Stream flow Characteristics" Netherlands and New York, Elsevier, p. 249.

Robinson, G.J. (1994), "The accuracy of digital elevation model data derived from digitized contour data." The Photogrammetric Record, 14, p. 805 – 814.

Report volume 1996, Master Plan of Pagladia Sub-basin, Brahmaputra Board, Ministry of Water Resources, Govt. of India, Chapter 1, p. 1.

Reinhart, R. (1997), "RADAR for meteorologists" Reinhart Publications.

Refsgaard, J.C. (1997), "Parameterisation, calibration and validation of distributed hydrological models." Journal of Hydrology, 198, p. 69 – 97.

Raje, D., Mujumdar, P.P. (2011), "A comparison of three methods of downscaling daily precipitation in Punjab region." Journal of hydrological processes, 25, p. 3575 – 3589.

Sherman, L. K. (1932), "Streamflow from rainfall by the unit graph method." Eng. News Rec., 108, p. 501–505.

Strahler, A. N. (1952), "Hypsometric (area-altitude) analysis of erosional topography." Bulletin of Geological Society of America, 63, p. 1117-1142.

Shuman, F.G. (1978), "Numerical Weather Prediction." Bulletin of American Meteorological Society, 59, p. 5 – 17.

Sauvageot, H. (1991), "RADAR meteorology" Artech house Inc, p. 315.

Saulnier, G.M., Obled, C., Beven, K. J. (1997), "Analytical compensation between DTM grid resolution and effective values of saturated hydraulic conductivity

within the TOPMODEL framework" Journal of Hydrological Process, 11, p. 1331 - 1346.

Shin, K.S., Chun, S.K., Lee, S.Y., Yoo, H.D., Lee, D.I., Xue, M., Brewster, K., Bassett, G., Park, S.K., Droegemeier, K.K. (1998), "Explicit real time operational prediction of deep convection over Korea." Conf. of American Meteorological Society, Phoenix AZ, p. 135 – 137.

Sarma A.K., Das M.M. (2001), " Mathematical Model for Simulating Flood Propagation on Downstream of River Dike, Proc. of International Conference on Mathematical Modelling, Roorkee, p. 569- 573.

Singh, V.P. (2003), "On the theories of Hydraulic Geometry." International Journal of sediment research, 18, p. 196 – 218.

Sivapalan, M., Blöschl, G. (2003). "Downward approach to hydrological prediction." Journal of Hydrological Processes, 17, p. 2101-2111.

Sarma A.K. (2004), "Hydraulic Structures (Chapter 12)" The book: Brahmaputra Basin Water Resources, Kluwer Academic Publisher of Netherland, p. 261 – 273.

Stevens, N.F., Wadge, G. (2004), "Towards operational repeat-Pass SAR interferometry at active volcanoes." Journal of *Natural Hazards*, **33**, p. 47-76.

Schulz, K., Seppelt, R., Zehe, E., Vogel, H.J., Attinger, S. (2006), "Importance of spatial structures in advancing hydrological sciences." Journal of Water Resource Research, 42, p. 1 – 4.

Sakamoto, T, Nguyen, N. V., Kotera, A., Ohno, O., Ishitsuka, N., Yokozawa, M. (2007), "Detecting temporal changes in the extent of annual flooding within the Cambodia and the Vietnamese Mekong Delta from MODIS time-series imagery." Journal of Remote Sensing of Environment, 109, p. 295 – 313.

Sanders, B.F. (2007), "Evaluation of on-line DEMs for flood inundation modelling." Journal of Advances in Water Resources, 30, p. 1831 – 1843.

Sole, A., Giosa, L., Nole, L., Medina, V. and Bateman, A. (2008), "Flood risk modelling with LiDAR technology." http://gits.ws/06articulous/paper/01friar08.

Sinha, R., Bapalu, G.V., Singh, L.K., Rath, B. (2008), "Flood risk analysis in Kosi river basin, North Bihar Using multi-parametric approach of Analytic Hierarchy Process (AHP)." Journal of Indian Society of Remote Sensing, 36, p. 293 – 307.

Shu-Hua Z., ZHANG, N.C., Zheng, B.L., ZHANG, Z.X. (2009), "Numerical simulation of tidal current and erosion and sedimentation in the Yangshan deep-water harbor of Shanghai." International Journal of Sediment Research, 24, p. 287 – 298.

Shi, Z.H., Chen, L., Feng, N., Qin, D., Cai, C. (2009), "Research on the SCS-CN initial abstraction ratio using rainfall-runoff event analysis in the Three Gorge Area, China." CATENA, 77, P. 1 – 7.

Schroter, K., Liort, X., Forero, C.V., Ostrowski, M., Torres, D.S. (2010), "Implications of Radar rainfall estimates uncertainty on distributed hydrological model predictions." Journal of Atmospheric Research, 100, p. 237 – 245.

Thieken, A.H., Lucke, A., Diekkruger, B., Richter, O. (1999), "Scaling input data by GIS for hydrological modelling." Journal of Hydrological Processes, 13, p. 611 – 630.

USACE, 1976 report on Flood Risk Management Programme (FRMP), United Nations Organization.

Varnes, D.J. (1984), "Landslide hazard Zonation: A review of principles and Practice" UNESCO Publication, ISBN: 92-3-101895-7.

Van, Z.J. (2001) "The Shuttle Radar Topography Mission (SRTM): a breakthrough in remote sensing of topography." Acta Astronautica, 48, p. 559–565.

Viessman, J.R.W., Lewis, G.L. (2008), "Introduction to Hydrology". Prentice Hall, Englewood Cliffs, New Jersey.

Wolman, M.G. (1971), "Evaluating alternative techniques for floodplain mapping." Journal of water Resource Research, 7, p. 1383 – 1392.

Wolock, D.M., Price, C.V. (1994), "Effects of digital elevation model map scale and data resolution on a topography based watershed model." Journal of Water Resource Research, 30, p. 3041 – 3052.

Wicker, L. J., Skamarock, W. C. (2002), "Time splitting methods for elastic models using forward time schemes.", Mon. Wea. Rev., 130, p. 2088–2097.

Wang, Y. (2004), "Using Landsat 7 TM data acquired days after a flood extent on a coastal floodplain." International Journal of Remote Sensing, 25, p. 959 – 974.

Wardah, T., Kamil, A.A., Hamid, S., Maisarah, W.W.I. (2011). "Quantitative precipitation forecast using MM5 and WRF models for Kelantan river basin." Journal of World academy of Science: Engineering and technology, 59, p. 2469 – 2473.

Wang, W., Yang, X., and Yao, T. (2012), "Evaluation of ASTER GDEM and SRTM and their suitability in hydraulic modelling of a glacial lake outburst flood in southeast Tibet." Journal of Hydrological Processes, 26, p. 213 - 225.

Xue, M., Droegemeier, K.K., Wong, V. (2000), "The Advanced Regional Prediction System (ARPS) – A multi scale non hydrostatic atmospheric simulation and prediction model. Part I: Model dynamics and verification." Journal of Meteorology and Atmospheric Physics, 75, p. 161 – 193.

Xue, M., Droegemeier, K.K., Wong, V., Shapiro, A., Brewster, K., Carr, F., Weber, D., Liu, Y. and Wang, D.H. (2001), "The Advanced Regional Prediction System (ARPS) - A multi-scale non hydrostatic atmospheric simulation and prediction tool." Journal of Atmospheric physics, 76, p. 143 – 165.

Xue, M., Wang, D., Gao, J., Brewster, K., Droegmeier, K.K. (2002), "The Advanced Regional Prediction System (ARPS), storm-scale numerical weather prediction and data assimilation." Journal of Meteorology and Atmospheric Physics, 82, p. 139 – 170.

Xu, H. (2006), Modification of normalised difference water index (NDWI) to enhance open water features in remotely sensed imagery." International Journal of Remote sensing, 27, p. 3025-3033.

Xu, X., Tan, Y., Yang, G., Li, H., Su, W. (2011), "Soil erosion in the three gorges reservoir area." Journal of Soil Research, 49, p. 212 – 222.

Yamakazi, Y., Orgas, D.M., Prior, V.M.M.S. and Pinto, P. (2005), "A MM5 extreme precipitation event forecast over Portugal." NCAR meso-scale model user workshop.

Zhang, W., Montgomery, D.R. (1994), "Digital Elevation Model grid size, Landscape representation and hydrologic simulations." Journal of Water Resource Research, 30, p. 1019 – 1028.

Zoppou, C. (2001), "Review of urban storm water models." Environmental Modeling Software, 3, p. 195 – 231.

Zheng, N., Takara, K., Tachikawa, Y., Kozan, O. (2008), "Analysis of Vulnerability to flood hazard based on land use and population distribution in the Huaihe River basin, China." Annuals of Disaster prevention Research Institute, Kyoto University, No. 51 B, 2008.